



HAL
open science

Early alterations of bile canaliculi dynamics and the rho kinase/myosin light chain kinase pathway are characteristics of drug-induced intrahepatic cholestasis

M.G. Burbank, Audrey Burban, Ahmad Sharaneek, R.J. Weaver, Christiane Guguen-Guillouzo, André Guillouzo

► To cite this version:

M.G. Burbank, Audrey Burban, Ahmad Sharaneek, R.J. Weaver, Christiane Guguen-Guillouzo, et al.. Early alterations of bile canaliculi dynamics and the rho kinase/myosin light chain kinase pathway are characteristics of drug-induced intrahepatic cholestasis. *Drug Metabolism and Disposition*, 2016, 44 (11), pp.1780–1793. 10.1124/dmd.116.071373 . hal-01398437

HAL Id: hal-01398437

<https://univ-rennes.hal.science/hal-01398437>

Submitted on 23 Oct 2017

HAL is a multi-disciplinary open access archive for the deposit and dissemination of scientific research documents, whether they are published or not. The documents may come from teaching and research institutions in France or abroad, or from public or private research centers.

L'archive ouverte pluridisciplinaire **HAL**, est destinée au dépôt et à la diffusion de documents scientifiques de niveau recherche, publiés ou non, émanant des établissements d'enseignement et de recherche français ou étrangers, des laboratoires publics ou privés.

Early alterations of bile canaliculi dynamics and the ROCK/MLCK pathway are characteristics of drug-induced intrahepatic cholestasis

Matthew G. Burbank, Audrey Burban, Ahmad Sharanek, Richard J. Weaver, Christiane Guguen-Guillouzo, André Guillouzo

Inserm UMR 991 Foie, métabolismes et cancer, Rennes, France (M.B., A.B., A.S., C.G-G., A.G.); Université Rennes 1, Rennes, France (M.B., A.B., A.S., C.G-G., A.G.); Biologie Servier, Gidy, France (M.B.); International Research Institute Servier, Suresnes, France (R. J. W.); Biopredic International, St Grégoire, Rennes, France (C.G-G.).

DMD # 71373

Bile canaliculi deformation by cholestatic drugs

Address correspondence to: Prof. André Guillouzo, INSERM U991, Faculté de Pharmacie.
2 avenue L. Bernard, 35043 Rennes cedex, France. Tel: (33)223234791. Fax:
(33)223235685. E-mail address: andre.guillouzo@univ-rennes1.fr

Number of text pages: 19

Number of tables: 4

Number of figures: 6

Number of references: 69

Number of words:

- **Abstract: 248**
- **Introduction: 753**
- **Discussion: 1714**

Non-standard abbreviations:

ALB, albumin; ALDOB, aldolase B; AMI, amiodarone; APAP, acetaminophen; BA, bile acid; BC, bile canaliculi; BOS, bosentan; BSEP, bile salt export pump; BUS, buspirone; CaM, calmodulin; CIM, cimetidine; CPZ, chlorpromazine; CsA, cyclosporine A; CYP3A4, cytochrome P450 3A4; DIC, diclofenac; DILI, drug-induced liver injury; DMSO, dimethyl sulfoxide; ENT, entacapone; FIA, fialuridine; GAPDH, glyceraldehyde-3-phosphate dehydrogenase; MDR1, multidrug resistance 1; MET, metformin; MLC, myosin-light-chain; MLC2, myosin light chain subunit-2; MLCK, myosin light chain kinase; SOD2, manganese-dependent superoxide dismutase; MRP2,3,4, multidrug resistance-associated proteins 2,3,4; MTT, methylthiazoletetrazolium; NEF, nefazodone; NTCP, Na⁺-taurocholate co-transporting

DMD # 71373

polypeptide; OATP-B, organic anion transporting polypeptide; PER, perhexiline; PHH, primary human hepatocytes; PIO, pioglitazone; ROCK, Rho-kinase; ROS, reactive oxygen species; RT-qPCR, real-time quantitative polymerase chain reaction; SCHH, sandwich-cultured human hepatocytes; TCA, taurocholic acid; TAC, tacrolimus; TOL, tolcapone; TRO, troglitazone; [³H]-TCA, [³H]-taurocholic acid; XIM, ximelagatran; Y-27632, 4-(1-aminoethyl)-N-(4-pyridyl) cyclohexanecarboxamide dihydrochloride.

DMD # 71373

Abstract

Intrahepatic cholestasis represents 20-40% of drug-induced injuries from which a large proportion remains unpredictable. We aimed to investigate mechanisms underlying drug-induced cholestasis and improve upon its early detection using human HepaRG cells and a set of 12 cholestatic and 6 non-cholestatic drugs. Bile canaliculi (BC) dynamics, Rho/myosin-light-chain (MLC) kinase pathway implication, efflux inhibition of taurocholate, a predominant BSEP substrate, and expression of the major canalicular and basolateral bile acids transporters were analyzed. We demonstrated 12 cholestatic drugs classified on the basis of reported clinical findings caused disturbances of both BC dynamics, characterized by either dilatation or constriction, and alteration of the ROCK/MLCK signalling pathway while non-cholestatic compounds, by contrast, have no effect. Co-treatment with Y-27632, a ROCK inhibitor, and calmodulin, a MLCK activator, reduced BC constriction and dilatation, respectively confirming the role of these pathways in intrahepatic drug-induced cholestasis. By contrast, inhibition of taurocholate efflux and/or human BSEP overexpressed in membrane vesicles (published data) was not observed with all cholestatic drugs and moreover examples of non-cholestatic compounds reportedly found to inhibit BSEP. Transcripts levels of major bile acids transporters were determined after 24h-treatment. *BSEP*, *NTCP* and *OATP-B* were down-regulated with most cholestatic and some non-cholestatic drugs while deregulation of *MRPs* was more variable, probably mainly reflecting secondary effects. Together, our results show cholestatic drugs consistently cause an early alteration of BC dynamics associated with modulation of the Rho/MLC kinases and these changes are more specific than efflux inhibition measurements alone as predictive non-clinical markers of drug-induced cholestasis.

DMD # 71373

Introduction

Many drugs have been reported to induce liver injury in a dose-dependent or -independent manner in humans. Due to their hepatotoxicity and idiosyncrasy, a large fraction has been removed from the market or put under warning box during the last decades. A frequent manifestation of drug-induced liver injury (DILI) is represented by intra-hepatic cholestasis which is characterized by impaired hepatocellular secretion of bile, resulting in accumulation of bile acids (BA), bilirubin and cholesterol (Padda et al. 2011). In several population-based studies on DILI, a cholestatic pattern has been found in 20-40% and a mixed cholestatic and hepatocellular injury pattern in 12-20% of patients (Lee 2003) with a large proportion of the drug-induced cholestatic cases reportedly unpredictable.

Early detection of DILI and more particularly cholestasis remains a real challenge for pharmaceutical industries and regulatory agencies. According to the European Medicines Agency guidelines on the investigation of drug interactions and the International Transporter Consortium (Zamek-Gliszczynski et al. 2012), inhibition of the bile salt export pump (BSEP), that plays a major role in bile acid canalicular transport (Jansen et al. 1999; Stieger 2010), should be evaluated during drug development when evidence of cholestatic liver injury has been observed in nonclinical safety studies or in human clinical trials (Kenna 2014). Indeed, many drugs reported to cause DILI have been identified as efflux transporters inhibitors (Morgan et al. 2010; Stieger 2010; Dawson et al. 2012; Pedersen et al. 2013), but a significant number of false positives has been found (Pedersen et al. 2013). Moreover, compounds known to interfere with BSEP function are often not associated with significant liver cell injury in preclinical animal models although they have been related to liver damage when administered to humans (Morgan et al. 2010; Dawson et al. 2012;) and many cholestatic drugs are not BSEP inhibitors (Pedersen et al. 2013).

Currently, various *in vivo* and *in vitro* biological approaches are used for studying BA transporters. Detection of cholestatic drugs can depend on the choice of the method and/or

DMD # 71373

the model and its species origin. Animal models including knockout, mutant models and whole tissues can be employed but *in vitro* systems are more frequently used, based on membrane and cell assays (Brouwer et al. 2013). Inverted vesicles derived from various non-transfected or transfected cell lines are widely used to analyze interactions between substrates and inhibitors with target transporters. However, a number of probe substrates and inhibitors are recommended for evaluation of human ATP-dependent transport into membrane vesicles. Polarized cells are standard models for evaluating drug transport. Primary hepatocytes appear to be the most appropriate cell model to mimic the hepatic uptake and efflux functions. However, freshly isolated and cryopreserved hepatocytes are not polarized, and in standard culture conditions they rapidly lose their functional activities and functional bile canaliculi (BC) (Guguen-Guillouzo and Guillouzo 2010). Rat hepatocyte couplets (Graf et al. 1984; Thibault et al. 1992) and primary rat and human hepatocytes in a sandwich configuration (Swift et al. 2010; Ellis et al. 2014) have been the most widely used *in vitro* cell models to analyze hepatic transport processes. Sandwich-cultured human hepatocytes (SCHH) recapitulate the polarized architecture but they frequently exhibit large inter-donor and *in vitro* time-dependent functional variations. An alternative to SCHH is the human HepaRG cell-line which expresses features characteristic of mature hepatocytes, exhibits typical functional BC and correctly polarized distribution of transport proteins, and produces BA at levels comparable to those measured in primary human hepatocyte cultures (Guguen-Guillouzo and Guillouzo 2010; Bachour-El Azzi et al. 2015; Sharanek et al. 2015).

The mechanisms underlying drug-induced intrahepatic cholestasis remain poorly understood. Besides the role of hepatobiliary transporter changes, other mechanisms, such as altered cell polarity, disruption of cell-to-cell junctions and cytoskeletal modifications, are believed to participate to the development of intrahepatic cholestasis. In normal hepatocytes BC undergo spontaneous contractions, which are essential for BA efflux (Arias et al. 1993) and alternations in myosin light chain (MLC2) phosphorylation and dephosphorylation are required for these contractions (Sharanek et al. 2016). Recently, we reported that cholestatic

DMD # 71373

drugs can cause *in vitro* early constriction or dilatation of BC associated with deregulation of the Rho-kinase/myosin-light-chain-kinase (ROCK/MLCK) pathway (Sharanek et al. 2016).

In the present work, we aimed to determine whether changes in BC dynamics and the ROCK/MLCK pathway are more representative targets of cholestatic drugs than the efflux transporters inhibition and whether these alterations could better discriminate cholestatic from non cholestatic compounds using human differentiated HepaRG cells. Our results showed that the 12 tested cholestatic drugs could cause BC constriction and dilatation associated with different disturbances of the ROCK/MLCK pathway.

DMD # 71373

Materials and methods

Reagents

Cyclosporine A (CsA), chlorpromazine (CPZ), nefazodone (NEF), tolcapone (TOL), diclofenac (DIC), perhexiline (PER), troglitazone (TRO), tacrolimus (FK-506) (TAC), amiodarone (AMI), acetaminophen (APAP), ximelagatran (XIM), metformin (MET), entacapone (ENT), buspirone (BUS), pioglitazone (PIO), cimetidine (CIM), 4-(1-aminoethyl)-N-(4-pyridyl) cyclohexanecarboxamide dihydrochloride (Y-27632) and methylthiazole tetrazolium (MTT) were purchased from Sigma (St. Quentin Fallavier, France). Fialuridine (FIA) was supplied by Carbosynth (Compton, U.K). Bosentan (BOS) was obtained from Sequoia Research Products (Pangbourne, U.K). Calmodulin (CaM) was provided from Merck Chemicals (Fontenay sous Bois, France). Phalloidin fluoprobe was purchased from Interchim (Montluçon, France). [³H]-taurocholic acid ([³H]-TCA) was supplied by Perkin Elmer (Boston, MA). Specific antibodies against phospho-myosin light chain 2 (ser19) and HSC70 were provided from Cell Signaling Technology (Schuttersveld, The Netherlands). Secondary antibodies were obtained from Invitrogen (Saint Aubin, France). Hoechst dye was from Promega (Madison, WI). Other chemicals were of the highest reagent grade.

Cell cultures and treatments

HepaRG cells were seeded at a density of 2.6×10^4 cells/cm² in Williams E medium supplemented with 2mm glutamax, 100μ/ml penicillin, 100μg/ml streptomycin, 10% Hyclone bovine fetal calf serum, 5μg/ml insulin, and 50μM hydrocortisone hemisuccinate. At confluence, after a 2-week cell proliferation phase, HepaRG cells were shifted to the same medium supplemented with 1.7% dimethyl sulfoxide (DMSO) for 2 additional weeks in order to obtain confluent differentiated cultures containing equal proportions of hepatocyte-like and progenitors/primitive biliary-like cells (Cerec et al. 2007). These differentiated hepatic cell cultures were used for analytical assays.

DMD # 71373

Primary human hepatocytes (PHH) were obtained from Biopredic International (St Gregoire, France). They were isolated by collagenase perfusion of histologically normal liver fragments from 3 adult donors undergoing resection for primary and secondary tumours (Guguen-Guillouzo et al. 1982). These three donors were caucasian males: 74-, 65-, and 71-year old for donor 1, 2 and 3, respectively. Primary cultures were obtained by seeding 1.5×10^5 hepatocytes per cm^2 onto plates in Williams E medium supplemented with 10% Hyclone bovine fetal calf serum, 100units/ μl penicillin, 100 $\mu\text{g}/\text{ml}$ streptomycin, 1 $\mu\text{g}/\text{ml}$ insulin, 2mM glutamine. The medium was discarded 12h after cell seeding, and cultures were thereafter maintained in serum-free medium. PHH cultures were used 3-4 days after cell seeding. For drug treatments, differentiated HepaRG cells and PHH were incubated in a medium containing 2% serum and 1% DMSO. The list and characteristics of tested drugs are displayed in Table 1. The drugs were divided into 3 groups according to their effects in clinic: well recognized as cholestatic (group 1), rarely cholestatic (group 2) and non cholestatic (group 3). The compounds were dissolved in DMSO or water and the final concentration of the solvent did not exceed 1%.

Cell viability

Cytotoxicity of the tested drugs was evaluated using the MTT colorimetric assay. Briefly, cells were seeded in 96- or 24-well plates and exposed to various concentrations of each compound in triplicate for 24h. After medium removal, 100 μl serum- and DMSO-free medium containing MTT (0.5mg/ml) was added to each well and incubated for 2h at 37°C. The water-insoluble formazan was dissolved in 100 μl of DMSO and absorbance was measured at 550nm (Aninat et al. 2006). IC₂₀ values (the concentrations causing 20% cytotoxicity) were calculated from the concentration-responses curves.

DMD # 71373

Time-lapse cell imaging

Phase-contrast images of HepaRG cells and PHH were captured every 10min, using time-lapse phase-contrast videomicroscopy. The inverted microscope Zeiss Axiovert 200M was equipped with a thermostatic chamber (37°C and 5% CO₂) to maintain the cells under normal culture conditions and with an Axiocam MRm camera with a 10x objective.

Determination of canalicular lumen surfaces

Canalicular lumen surfaces appeared bright (white) and the hepatocytes/biliary cells denser (black) using a phase-contrast microscope Zeiss Axiovert 200M. Brightness parameters were adjusted to better distinguish between white and black densities and analysis was performed on at least 4 images per condition per well. White canalicular lumen was then quantified using the image J software every 10min for 24h. Data obtained during the first 4h with all tested compounds are presented and BC quantification is expressed as percent of the control (Supplement Figure 1).

MLCK and ROCK modulation

MLCK and ROCK implication in BC deformations was determined by the use of calmodulin (CaM) and Y-27632, two specific modulators. HepaRG cells were treated with CaM, a specific MLCK activator, and Y-27632, a selective ROCK inhibitor, in the presence or absence of dilators and constrictors, respectively (Sharanek et al. 2016). BC alterations after co-treatment were quantified and compared to treatment with the modulator alone as described above.

Taurocholic acid clearance

Cells were first exposed to 43.3nM [³H]-TCA for 30min to induce its intracellular accumulation, then washed with standard buffer and incubated with the tested compounds for 2h in a standard buffer with Ca²⁺ and Mg²⁺. After the incubation time, cells were washed

DMD # 71373

and scraped in 0.5N NaOH and the remaining radiolabeled substrate was measured through scintillation counting to determine [³H]-TCA clearance. [³H]-TCA clearance was determined based on its accumulation in the cell layers (cells + BC) and calculated relative to the control using the following formula: [³H]-TCA clearance = ($\frac{[\text{³H]-TCA accumulation in (cells + BC)}_{\text{Control}} * 100}{[\text{³H]-TCA accumulation in cell layers}_{\text{Tested compound}}}$) (Sharanek et al. 2016).

Real-time quantitative polymerase chain reaction (RT-qPCR) analysis.

Total RNA was extracted from 10⁶ HepaRG cells with the SV total RNA isolation system (Promega). RNAs were reverse-transcribed into cDNA and RT-qPCR was performed using a SYBR green mix. Primer pairs sequences are listed here: *GAPDH* (ID 2597), forward, 50-ttcaccaccatggagaaggc-30: reverse, 50-ggcatggactgtggcatga-30; *BSEP* (ID 8647), forward, 50-tgatcctgatcaaggaagg-30: reverse, 50-tggctcctgggaacaattc-30; *NTCP* (ID 6554), forward, 50-gggacatgaacctcagatt-30: reverse, 50-cgttgattgaggacgat-30; *OATP-B* (ID 6579), forward, 50-tgattggtatggggctatc-30: reverse, 50-catatcctagggctggtgt-30; *MRP2* (ID 1244), forward, 50-tgagcaagttgaaacgcacat-30: reverse, 50-agctctctcctgccgtctct-30; *MRP3* (ID 8714), forward, 50-gtccgcagaatggacttgat-30: reverse, 50-tcaccactggggatcatt-30; *MRP4* (ID 10257), forward, 50-gctcaggtgcctatgtgct-30: reverse, 50-cggttacaattcctcctcca-30; *ALB* (ID 213), forward, 50-gctgtcatctctgtgggctgt-30: reverse, 50-actcatgggagctgctggttc-30; *ALDOB* (ID 229), forward, 50-tgcgcccagtagaagaaggacgggtg-30: reverse, 50-ctcaagatctcggacggctg-30. *CYP3A4* (ID 1576), forward, 50-tcagcctggtgctcctctatctat-30: reverse, 50-tccagggcccacacctctgcct-30; *SOD2* (ID 6648), forward, 50-acaggccttattcactgct-30: reverse, 50-cagcataacgatcgtggtt-30.

Western blotting analysis of p-MLC2

HepaRG cells were treated with the tested compounds for 1, 2 and 3h at a concentration causing BC alteration, then washed with cold phosphate-buffered saline and finally re-suspended in cell lysis buffer supplemented with protease and phosphatase inhibitors

DMD # 71373

(Roche, Mannheim, Germany). Aliquots containing equivalent total protein content, as determined by the Bradford procedure with bovine serum albumin as the standard, were subjected to sodium dodecyl sulfate/12% polyacrylamide gel electrophoresis, electro-transferred to immobilon-p membranes, and incubated overnight with primary antibodies directed against p-MLC2 and HSC70. After incubation with a horseradish peroxidase-conjugated anti-mouse/rabbit antibody (ThermoFisher Scientific, Waltham, MA), membranes were incubated with a chemiluminescence reagent (Millipore, Billerica, MA) and bands were visualized and quantified by densitometry with fusion-CAPT software (Vilber Lourmat, Collegien, France).

Statistical analysis

One-way Anova with multiple comparison test (graphpad prism 6.00) was performed to compare time-dependent MLC2 phosphorylation in different samples. Data were considered significantly different when $*P < 0.05$. The student t test was applied to compare values of BC quantification between treated and corresponding co-treated cultures (with CaM or Y-27632). Data were considered as significantly different when $^{\#}P < 0.001$. The student t test was also applied to compare values of BA clearance and mRNA levels between treated and corresponding control cultures. Data were considered as significantly different when $*P < 0.05$, $**P < 0.01$ and $***P < 0.001$. Each value corresponded to the mean \pm standard error (SEM) of three independent experiments.

DMD # 71373

Results

Cytotoxicity determination

Experiments were performed to firstly calculate IC₂₀ values for each compound after a 24h treatment of HepaRG cells using the MTT assay (Table 2). Then, three concentrations were tested for further experiments, the highest corresponding to the IC₂₀ value. IC₁₀ or IC₂₀ values are commonly selected for use in early *in vitro* toxicology studies (Liguori, et al. 2008; Pomponio et al. 2015). When IC₂₀ values could not be determined because of absence of toxicity, higher concentrations were tested. The IC₂₀ values and/or final selected maximum concentrations tested are displayed in Table 2.

Bile canaliculi dynamics

BC contractions are essential for clearance of BAs; they are characterized by repeated opening and closing processes (Sharanek et al. 2016). We examined BC dynamics in living cells by time-lapse imaging during at least 12h after addition of the tested compounds. Depending on the drug, BC showed constriction, dilatation or no change. The 5 compounds from group 1 caused early alterations of BC, usually starting after 1h exposure of HepaRG cells (Figure 1). As previously reported (Sharanek et al. 2016), CPZ (50µM) and CsA (50 µM) induced constriction while BOS (100 µM) caused dilatation of BC. The two other cholestatic compounds from group 1 (NEF and TRO) and 4 rarely cholestatic compounds from group 2 (DIC, ENT, PER, TAC) also caused morphological alterations of BC at the same range of concentrations, either constriction with NEF (75µM), PER (20µM) and TRO (50µM) (Supplemental video 1) or dilatation with ENT (100µM) (Supplemental video 2), DIC (200µM) and TAC (50µM) (Figure 1A and B). Two other compounds from group 2, MET and CIM, also caused alterations of BC dynamics but at much higher although non cytotoxic concentrations, i.e. constriction and dilatation at 3 and 4mM respectively (Figure 1B).

DMD # 71373

Noticeably, differential time- or concentration-dependent BC alterations were evidenced with some cholestatic compounds. Thus, among the 5 constrictors from group 1, only CsA caused dilatation of BC at low concentrations (10 μ M) (Figure 1C). Interestingly, one group 2 compound, TOL (100 μ M), showed dilatation during the first hour followed by constriction of BC during the following hours of treatment (Figure 1D). By contrast, ENT, a dilatator from the same therapeutic family as TOL, caused strong dilatation starting within the first hour without any constriction during the following hours (Figure 1B). All other tested compounds, namely XIM, AMI, APAP, FIA, BUS and PIO (group 3), did not alter BC dynamics at non cytotoxic concentrations (Figure 2E; Supplemental video 3).

Morphological canalicular alterations induced by the tested compounds were quantified by measuring the canalicular surface using the image J software every 10min for 24h. Data obtained during the first 3h with all tested compounds are displayed in Figure 1F-I. When observed several altered BC were detected whatever the selected culture area or the tested drug. Interestingly, the results were comparable to those previously obtained using the canalicular distribution of zona occludens-1 protein to measure BC areas (Sharanek et al. 2016); e.g. BOS caused 1.5-fold increase in BC surfaces using either method.

Interestingly, constrictions appeared to be irreversible while dilatations were only transient, as seen with TOL. Noticeably, AMI showed an unspecific increase in BC surface quantification starting after 1h due to appearance of intracytoplasmic vesicles corresponding to induction of phospholipidosis (Figure 1E). Drug effects on BC structures are summarized in Supplemental Table 1.

ROCK and MLCK alterations with cholestatic drugs

The myosin light chain subunit-2 (MLC2), the regulatory subunit of myosin 2, that is predominantly distributed in the pericanalicular region of hepatocytes, is known as a target of ROCK; its phosphorylation/dephosphorylation reflects the dynamic rhythm of BCs and was

DMD # 71373

found to be impaired by CPZ, CsA and BOS (Sharanek et al. 2016). Based on this previous study, we analyzed the 18 compounds at 3 critical time-points (i.e. 1, 2 and 3h) by western blotting. However, we first verified with 6 compounds that similar alterations of MLC2 phosphorylation occurred after 30min whatever the compound (Supplemental Figure 2). Western blots analysis of MLC2 showed an increased phosphorylation tendency between 1 and 3 hours with constrictors (i.e. CPZ, CsA, PER, NEF, TRO and MET) and inversely dephosphorylation tendency with dilatators (i.e. TAC, BOS, CIM and DIC) (Figure 2A). Depending on the compound, either a constrictor or a dilatator, large individual quantitative differences were observed in their effects (Figure 2B). The potent constrictors, PER, TRO and NEF, showed a much higher rate of phosphorylation than metformin after 3h treatment (Figure 2A, B). Interestingly, ENT showed a decrease of MLC2 phosphorylation during BC dilatation while TOL did not show any significant change, likely due to rapid morphological changes of BC from dilatation to constriction after one hour treatment (Figure 2B). All non cholestatic drugs did not significantly affect MLC2 phosphorylation/dephosphorylation (Figure 2C, D).

To further analyze alterations of BC dynamics by cholestatic compounds, involvement of ROCK and MLCK was investigated using Y-27632, a specific inhibitor of ROCK, and CaM, a specific MLCK activator. Y-27632 (10 μ M) caused BC dilatation whereas CaM (5 μ M) alone, caused no BC alteration (Figure 3A). Alteration of BC size after co-treatment with a drug and CaM or Y-27632 was quantified and compared to the drug treatment alone. As expected, a co-treatment with CaM reduced BC dilatation induced by the dilatators (i.e. BOS, DIC, CIM and TAC) (Figure 3B and F). By contrast, co-treatment with Y-27632 partly counteracted the early phase of constriction induced by the constrictors (i.e. TRO, NEF, PER and MET) (Figure 3C and D). TOL showed a lower dilatation during the first hour when co-treated with CaM and less constriction after 1h when co-treated with Y-27632 whereas ENT showed a much lower dilatation in the presence of CaM (Figure 3E). Interestingly, a co-treatment with

DMD # 71373

BOS and Y-27632 showed an increase in dilatation extent in comparison with BOS or Y-27632 alone (Figure 3G).

Taurocholic acid clearance

The influence of all tested drugs on efflux of [³H]-TCA, a predominant BSEP substrate, was assessed in HepaRG cells maintained in a standard buffer. Cells were first incubated with [³H]-TCA for 30min and then treated for 2h with all drugs at three different concentrations, the highest causing BC alterations. [³H]-TCA clearance, reflecting BAs accumulation in HepaRG hepatocytes and thus the cholestatic potential was determined by quantification of intracellular accumulation of radiolabeled TCA. The results are displayed in Figure 4. Two categories of compounds could be distinguished. The first one was composed of 8 compounds that caused a dose-dependent decrease in TCA clearance after 2h treatment; it included the 5 group 1 cholestatic drugs (i.e. NEF, TRO, BOS, CPZ and CsA) as well as 3 drugs of group 2 (i.e. PER, TOL and TAC). The second category was composed of the other 10 drugs that did not inhibit TCA efflux at the concentrations used; it included 4 drugs of group 2 (i.e. DIC, ENT, MET and CIM) and the 6 drugs that are classified as non cholestatic *in vivo* (i.e. XIM, AMI, APAP, FIA, BUS and PIO). Noticeably, DIC caused a concentration-dependent increase of TCA clearance, reaching 4-fold at 200µM.

Modulation of bile acids transporter expression

Genes encoding the major BA transporters can also be deregulated by cholestatic drugs (Pauli-Magnus and Meier 2006) and the deregulation of their mRNA expression is usually linked to their activity (Bramow et al. 2001). Six major genes encoding either efflux (*BSEP*, *MRP2*, *MRP3* and *MRP4*) or uptake (*NTCP*, *OATP-B*) transporters were analyzed by RT-qPCR after a 24h treatment with 3 concentrations of each tested drug. Different patterns depending on the compound and the tested concentration, were evidenced and are shown in Table 3 and supplemental Figures 3-8. Both *BSEP* and *NTCP* were strongly repressed by all

DMD # 71373

group 1 cholestatic compounds. In addition, *OATP-B* was repressed by CsA, BOS and NEF while *MRP2*, *MRP3* and *MRP4* were overexpressed only by CsA. Most compounds of group 2, i.e. TOL, DIC, PER, MET, CIM and TAC, also repressed *BSEP*, *NTCP* and *OATP-B*. Moreover, *MRP2*, *MRP3* and *MRP4* were upregulated by TAC. In addition, *MRP2* was up-regulated by DIC and *MRP3* was down-regulated by PER. Noticeably, none of the tested transporters was significantly deregulated by ENT. Some BA transporters were also deregulated by non cholestatic compounds. Thus, BUS down-regulated *BSEP* and *NTCP* while PIO and AMI inhibited *BSEP* and *NTCP* expression. In addition, transcripts of four other genes, i.e. *ALB*, *ALDOB*, *CYP3A4* and *SOD2*, were also measured (supplemental Table 2). A slight or significant decrease in the expression of the liver-specific genes, *ALB* and *ALDOB*, was also observed with most drugs, that likely reflected cell adaptation or some cytotoxicity after a 24h treatment and not a direct drug-induced cholestatic effect. Induction of *CYP3A4* mRNAs with CPZ and their inhibition by CsA, TAC and BOS agreed with previous reports. *SOD2* mRNA expression was increased with CsA and CPZ and was not altered with controls compounds.

Comparative analysis of BC dynamics in primary human hepatocytes

Hepatocytes from 3 different donors were analyzed by phase-contrast cell imaging. Similar results as those described with HepaRG hepatocytes were obtained within the first hours of drug exposure, i.e. BC constriction with CPZ, CsA, NEF and TRO (Figure 5A) as well as with TOL after 2h, and BC dilatation with TOL (between 1-2h), ENT, DIC and BOS (Figure 5B); however, these effects were not observed in cells from all donors with DIC, ENT and TAC. Moreover, the rarely cholestatic drug PER that caused BC constriction in HepaRG cells, did not alter BC structures in any of the 3 PHH populations (Figure 5C). As expected, the non cholestatic drug FIA was ineffective. The time-course of appearance of BC alterations was approximately the same for all the cholestatic compounds but the extent of dilatation appeared to be reduced compared to that observed in HepaRG cells.

DMD # 71373

Discussion

Both BC dynamics and ROCK/MLCK activities can be impaired by cholestatic drugs (Sharanek et al. 2016). In the current study, we demonstrated by using a set of 18 cholestatic and non cholestatic compounds that the 12 drugs classified cholestatic on the basis of reported clinical findings caused disturbances of both BC dynamics and the ROCK/MLCK pathway. By contrast, non cholestatic compounds exhibited no effect on these pathways. Comparison of these data with TCA efflux showed some cholestatic drugs were ineffective or enhanced TCA clearance while some non cholestatic exerted an inhibitory effect.

Drug-induced impairment of BC dynamics can result in either early constriction or dilatation of the canalicular lumen. These morphological changes were observed with the two groups of cholestatic drugs, i.e either well-recognized as causing clinical cholestasis or responsible of rare cases of clinical cholestasis (Table 1). BC constriction was irreversible, representing a terminal step leading to cell death while dilatation could be reversible and did not impede, at least within 24h, cell survival. Interestingly, the two types of BC alterations could be observed with some drugs, showing either time- concentration-dependency. TOL caused first dilatation and later on constriction while CsA caused dilatation at low and constriction at high concentrations. However, other BC constrictors, i.e. CPZ, NEF, PER and TRO did not show clear evidence of dilatation prior to constriction or differences in the effects on BC dynamics at lower concentrations or shorter time. Since a cholestatic liver usually develops after chronic drug administration in patients and is characterized by dilatated BC (Imanari, et al. 1981; Watanabe et al. 1991; Chung et al. 2002;) experiments are on-going to determine whether dilatation of BC could occur after prolonged repeated treatments with constricting drugs at lower concentrations. No BC alteration was observed with the 6 non cholestatic drugs. Noticeably, additional non cholestatic drugs have been tested, especially ambrisentan, a member of the endothelin receptor antagonists family as BOS, and ibuprofen and were found to be similarly ineffective (data not shown).

DMD # 71373

Noteworthy, BC constriction and dilatation were associated with different alterations of the ROCK/MLCK pathway. Activation of the ROCK pathway and inhibition of the MLCK pathway associated with increased phosphorylation and dephosphorylation of MLC2 were observed with constrictors and dilators respectively (Figure 6). Importantly, differential quantitative effects were observed, supporting the conclusion that cholestatic drugs can act by different mechanisms, involving different targets on the ROCK/MLCK pathway (Sharanek et al. 2016). The involvement of MLC2 in the occurrence of BC constriction or dilatation was also demonstrated by using Y-27632, a specific ROCK inhibitor, and CaM, a specific MLCK activator, which caused inhibition of BC constriction and dilatation respectively, giving support to the conclusion that disturbances of the ROCK/MLCK pathway preceded alterations of BC dynamics. Interestingly, BOS combined with Y-27632 had an additive effect on BC dilatation showing that both acted via distinct MLCK and ROCK enzymatic targets (Figure 3G).

Drug inhibition studies of BSEP have mostly been performed using membrane vesicles overexpressing BSEP (Morgan et al. 2010). Although PHH represent a more relevant physiological *in vitro* model they have been only rarely used (Kostrubsky 2006; Swift et al. 2010; Pedersen et al. 2013). A large proportion of cholestatic drugs has been identified as BSEP inhibitors (Morgan et al. 2010; Stieger 2010; Dawson et al. 2012; Pedersen et al. 2013), but a significant number of false positives has been found, using either vesicle assays or SCHH (Pedersen et al. 2013). Using the TCA clearance assay we also found that not all cholestatic drugs are inhibitors of TCA clearance. Indeed, compared to deformation of BC associated with disruption of the ROCK/MLCK pathway induced by the 12 cholestatic drugs and not by the 6 non cholestatic drugs, alteration of TCA clearance was observed only with 4/7 drugs known to rarely cause cholestasis in clinic, i.e. DIC, ENT, MET and CIM. Noticeably, if DIC and ENT inhibit BSEP using transfected vesicles, MET and CIM are not classified or only weakly shown to be inhibitors of BSEP (Morgan et al. 2010). Moreover, the potent cholestatic drug CPZ was not detected as a BSEP inhibitor using transfected vesicles

DMD # 71373

(Pedersen et al. 2013) whereas it appeared as a BC constrictor and an inhibitor of TCA efflux in the current study. This discrepancy could be attributed to CPZ-induced generation of ROS that cannot be observed with transfected vesicles (Anthérieu et al. 2013). Two additional major differences were evidenced between transfected cells and TCA clearance assays: we observed inhibition of TCA clearance and BC deformation with TOL and no change with PIO while opposite data were reported with transfected vesicles (Pedersen et al. 2013; Morgan et al. 2010). Noticeably, PIO has been classified as either rarely cholestatic (May et al. 2002) or non cholestatic (Pedersen et al. 2013) and as a potent BSEP inhibitor (Morgan et al. 2010; Dawson et al. 2012) or not (Kaimal et al. 2009; Pedersen et al. 2013) using transfected vesicles. However, in Pedersen's work PIO at 50 μ M did not significantly inhibit TCA efflux in SCHH. Our results agreed with this finding; at 100 μ M, PIO had no effect on TCA efflux or BC dynamics. Together, these data clearly emphasize the importance of both cell model-based systems and assays to estimate BSEP inhibition. Obviously, in our experimental whole-cell system, TCA efflux could not be considered as reflecting only BSEP activity. Indeed, TCA clearance was reduced to around 20% of control values by CsA. This strong inhibition could be due not only to an inhibition of canalicular efflux, but also to an inhibition of basolateral efflux. By contrast, a dose-dependent increase in TCA efflux was obtained with DIC, likely reflecting an enhanced basolateral efflux and/or a reduced influx activity. Moreover, with some drugs whether cholestatic or not (for example BUS), only a slight increase in TCA efflux was observed at low concentrations while at higher concentrations efflux levels were comparable to those measured in control HepaRG cell cultures, confirming previously reported concentration-dependent effects of drugs on TCA efflux using SCHH (Kostrubsky 2006). With the two compounds, MET and CIM, high non-cytotoxic concentrations were required to observe changes in BC dynamics while TCA efflux levels were comparable to those measured in controls but significantly decreased with low drug concentrations. By contrast, ENT did not inhibit TCA efflux at any of the concentrations tested. Together, these data support the conclusion that not all cholestatic drugs induce accumulation of TCA in

DMD # 71373

HepaRG cells and that its clearance can be modulated by different mechanisms other than direct alteration of BSEP activity.

Most studies have focused on interactions between drugs and BSEP without considering perturbation of expression of this transporter. Recently, one group (Garzel et al. 2014) analysed 30 drugs for their ability to perturb *BSEP* expression in PHH cultures after 24h treatment and classified them into 3 categories according to their capacity to strongly (>60%), moderately (20-60%) or not repressing the transporter. In the current study, we analysed four of these compounds. Similarly, we found a strong repression of *BSEP* expression with TRO and BOS that were tested at comparable concentrations but we evidenced a strong repression with NEF and CsA which were tested at higher concentrations. As shown here, the effects of cholestatic and non cholestatic drugs on BA transporters expression depended on drug concentration and the tested transporter (Supplemental Figure 3A). Noteworthy, most cholestatic drugs repressed *BSEP*, *NTCP* and *OATP-B* at concentrations that caused BC deformations, suggesting that *in vitro* experimental conditions (drug concentrations, *in vitro* model,...) are critical for obtaining correct results. The three BA transporters were also repressed by some non cholestatic drugs. Interestingly, it has been found that in human cholestatic liver, down-regulation of transporters also occurs at the mRNA level as observed for *BSEP*, *NTCP*, *OATP* (Zollner et al. 2001). More variable results were obtained with *MRPs* (Table 3). The most important changes were induction of *MRP2-4* with CsA and TAC and of *MRP2* with DIC. *MRP3* up-regulation has been described as a compensatory mechanism to BA accumulation in cholestatic rat liver (Donner and Keppler 2001). Since transcripts levels were measured 24h after drug addition, their changes reflected more likely secondary effects rather than direct and specific drug effects.

Interestingly, different responses were obtained with drugs of a same family as observed with TOL and ENT (as described above) as well as CsA and TAC that caused BC constriction

DMD # 71373

and dilatation respectively. TAC has been reported to cause rare cases of cholestasis in infants. Accordingly, it induced dilatation at only 50 μ M in this study. Since TAC is used at 10 to 100-fold lower therapeutic doses than CsA, the absence of hepatotoxic and cholestatic effects at concentrations up to 25 μ m fully agreed with its safety reported in clinic (Mihatsch et al. 1998). Accordingly, considering the C_{max} values measured in patients, i.e. 1.15 and 0.09 μ M for CsA and TAC respectively, cholestatic concentrations are expected to be reached normally only in patients treated with CsA. However, considering the 12 tested cholestatic drugs, no direct correlation could be established between C_{max} (Table 2) and their *in vitro* concentrations inducing BC deformation, confirming data reported with BSEP inhibition assays on a large set of compounds (Dawson et al. 2012; Köck et al. 2014).

BC deformation was also investigated in PHH cultures from 3 donors treated with some of the tested compounds. If both BC constriction and dilatation were induced by all cholestatic drugs except PER, donor-donor differences were observed. Only 4/8 tested cholestatic compounds were found to cause alterations or no changes of BC structures in the 3 hepatocyte populations. Among the factors that could explain donor differences were variations in drug metabolism and detoxification capacity and/or BA transporters levels. Nevertheless, these data with PHH confirm those obtained with HepaRG cells and support the suitability of this model as a reproducible, easy to use liver cell model for screening and mechanistic studies for the identification of on drug-induced cholestasis.

In summary, early BC deformations resulting in constriction or dilatation of the canalicular lumen associated with alterations of the ROCK/MLCK pathway were observed with all tested cholestatic drugs, including those which are not BSEP inhibitors (Table 4). Together, our results favour the conclusion that alterations of BC dynamics with the involvement of the ROCK/MLCK pathway are more specific predictive markers than TCA clearance and direct BSEP inhibition to screen the cholestatic potential of new chemical entities.

DMD # 71373

Acknowledgment

We thank R. Le Guevel from the ImPACcell platform (Biosit) for imaging analysis.

Authorship Contributions

Participated in research design: Matthew G. Burbank, Audrey Burban, Ahmad Sharaneq, André Guillouzo.

Conducted experiments: Matthew G. Burbank

Performed data analysis: Matthew G. Burbank, André Guillouzo, Christiane Guguen-Guillouzo, Richard J. Weaver

Wrote or contributed to the writing of the manuscript: Matthew G. Burbank, André Guillouzo, Richard J. Weaver

DMD # 71373

References

- Aninat, Caroline, Amélie Piton, Denise Glaise, Typhen Le Charpentier, Sophie Langouët, Fabrice Morel, Christiane Guguen-Guillouzo, and André Guillouzo. 2006. Expression of Cytochromes P450, Conjugating Enzymes and Nuclear Receptors in Human Hepatoma HepaRG Cells. *Drug Metabolism and Disposition: The Biological Fate of Chemicals* 34 (1): 75–83.
- Anthérieu, Sébastien, Alexandra Rogue, Bernard Fromenty, André Guillouzo, and Marie-Anne Robin. 2011. Induction of Vesicular Steatosis by Amiodarone and Tetracycline Is Associated with up-Regulation of Lipogenic Genes in HepaRG Cells. *Hepatology (Baltimore, Md.)* 53 (6): 1895–1905.
- Anthérieu, Sébastien, Pamela Bachour-El Azzi, Julie Dumont, Ziad Abdel-Razzak, Christiane Guguen-Guillouzo, Bernard Fromenty, Marie-Anne Robin, and André Guillouzo. 2013. Oxidative Stress Plays a Major Role in Chlorpromazine-Induced Cholestasis in Human HepaRG Cells. *Hepatology (Baltimore, Md.)* 57 (4): 1518–29.
- Arias, Irwin M., Mingxin Che, Zenaida Gatmaitan, Cynthia Leveille, Toshirou Nishida, and Marie St. Pierre. 1993. The Biology of the Bile Canaliculus, 1993. *Hepatology* 17 (2): 318–29.
- Bachour-El Azzi, Pamela, Ahmad Sharaneq, Audrey Burban, Ruoya Li, Rémy Le Guével, Ziad Abdel-Razzak, Bruno Stieger, Christiane Guguen-Guillouzo, and André Guillouzo. 2015. Comparative Localization and Functional Activity of the Main Hepatobiliary Transporters in HepaRG Cells and Primary Human Hepatocytes. *Toxicological Sciences: An Official Journal of the Society of Toxicology* 145 (1): 157–68.
- Banks, Alpha T., Hyman J. Zimmerman, Kamal G. Ishak, and John G. Harter. 1995. Diclofenac-Associated Hepatotoxicity: Analysis of 180 Cases Reported to the Food and Drug Administration as Adverse Reactions. *Hepatology* 22 (3): 820–27.

DMD # 71373

- Bramow, S., P. Ott, F. Thomsen Nielsen, K. Bangert, N. Tygstrup, and K. Dalhoff. 2001. Cholestasis and Regulation of Genes Related to Drug Metabolism and Biliary Transport in Rat Liver Following Treatment with Cyclosporine A and Sirolimus (Rapamycin). *Pharmacology & Toxicology* 89 (3): 133–39.
- Brouwer, K. L. R., D. Keppler, K. A. Hoffmaster, D. a. J. Bow, Y. Cheng, Y. Lai, J. E. Palm, B. Stieger, R. Evers, and International Transporter Consortium. 2013. *In Vitro* Methods to Support Transporter Evaluation in Drug Discovery and Development. *Clinical Pharmacology and Therapeutics* 94 (1): 95–112.
- Cerec, Virginie, Denise Glaise, Delphine Garnier, Serban Morosan, Bruno Turlin, Bernard Drenou, Philippe Gripon, Dina Kremsdorf, Christiane Guguen-Guillouzo, and Anne Corlu. 2007. Transdifferentiation of Hepatocyte-like Cells from the Human Hepatoma HepaRG Cell Line through Bipotent Progenitor. *Hepatology (Baltimore, Md.)* 45 (4): 957–67.
- Chu, Xiao-Yan, Kelly Bleasby, Jocelyn Yabut, Xiaoxin Cai, Grace Hoyee Chan, Michael J. Hafey, Shiyao Xu, et al. 2007. Transport of the Dipeptidyl Peptidase-4 Inhibitor Sitagliptin by Human Organic Anion Transporter 3, Organic Anion Transporting Polypeptide 4C1, and Multidrug Resistance P-Glycoprotein. *The Journal of Pharmacology and Experimental Therapeutics* 321 (2): 673–83.
- Chung, Kyu Won, Nam Ik Han, S. K. Yoon, S. W. Nam, Y. S. Lee, J. Y. Han, H. S. Sun, S. W. Choi, and B. M. Ahn. 2002. Increased Microfilaments in Hepatocytes and Biliary Ductular Cells in Cholestatic Liver Diseases. *Journal of Korean Medical Science* 17 (6): 795–800.
- Dawson, Sarah, Simone Stahl, Nikki Paul, Jane Barber, and J. Gerald Kenna. 2012. *In Vitro* Inhibition of the Bile Salt Export Pump Correlates with Risk of Cholestatic Drug-Induced Liver Injury in Humans. *Drug Metabolism and Disposition: The Biological Fate of Chemicals* 40 (1): 130–38.

DMD # 71373

- Dhillon, Sohita, and Gillian M. Keating. 2009. Bosentan: A Review of Its Use in the Management of Mildly Symptomatic Pulmonary Arterial Hypertension. *American Journal of Cardiovascular Drugs: Drugs, Devices, and Other Interventions* 9 (5): 331–50.
- Donner, M. G., and D. Keppler. 2001. Up-Regulation of Basolateral Multidrug Resistance Protein 3 (Mrp3) in Cholestatic Rat Liver. *Hepatology (Baltimore, Md.)* 34 (2): 351–59.
- Dykens, James A., Joseph D. Jamieson, Lisa D. Marroquin, Sashi Nadanaciva, Jinghai J. Xu, Margaret C. Dunn, Arthur R. Smith, and Yvonne Will. 2008. In Vitro Assessment of Mitochondrial Dysfunction and Cytotoxicity of Nefazodone, Trazodone, and Buspirone. *Toxicological Sciences: An Official Journal of the Society of Toxicology* 103 (2): 335–45.
- Ellis, L. C. J., M. H. Grant, G. M. Hawksworth, and R. J. Weaver. 2014. Quantification of Biliary Excretion and Sinusoidal Excretion of 5(6)-Carboxy-2',7'-Dichlorofluorescein (CDF) in Cultured Hepatocytes Isolated from Sprague Dawley, Wistar and Mrp2-Deficient Wistar (TR(-)) Rats. *Toxicology in Vitro: An International Journal Published in Association with BIBRA* 28 (6): 1165–75.
- Fattinger, K., C. Funk, M. Pantze, C. Weber, J. Reichen, B. Stieger, and P. J. Meier. 2001. The Endothelin Antagonist Bosentan Inhibits the Canalicular Bile Salt Export Pump: A Potential Mechanism for Hepatic Adverse Reactions. *Clinical Pharmacology and Therapeutics* 69 (4): 223–31.
- Feuer, G., and C. J. Di Fonzo. 1992. Intrahepatic Cholestasis: A Review of Biochemical-Pathological Mechanisms. *Drug Metabolism and Drug Interactions* 10 (1-2): 1–161.
- Fisher, Alexander, James Croft-Baker, Michael Davis, Patrick Purcell, and Allan J. McLean. 2002. Entacapone-Induced Hepatotoxicity and Hepatic Dysfunction. *Movement Disorders: Official Journal of the Movement Disorder Society* 17 (6): 1362–65; discussion 1397–1400.

DMD # 71373

- Fromenty, B., and D. Pessayre. 1995. Inhibition of Mitochondrial Beta-Oxidation as a Mechanism of Hepatotoxicity. *Pharmacology & Therapeutics* 67 (1): 101–54.
- Garzel, Brandy, Hui Yang, Lei Zhang, Shiew-Mei Huang, James E. Polli, and Hongbing Wang. 2014. The Role of Bile Salt Export Pump Gene Repression in Drug-Induced Cholestatic Liver Toxicity. *Drug Metabolism and Disposition: The Biological Fate of Chemicals* 42 (3): 318–22.
- Graf, J., A. Gautam, and J. L. Boyer. 1984. Isolated Rat Hepatocyte Couplets: A Primary Secretory Unit for Electrophysiologic Studies of Bile Secretory Function. *Proceedings of the National Academy of Sciences of the United States of America* 81 (20): 6516–20.
- Guguen-Guillouzo, C., J. P. Champion, P. Brissot, D. Glaise, B. Launois, M. Bourel, and A. Guillouzo. 1982. High Yield Preparation of Isolated Human Adult Hepatocytes by Enzymatic Perfusion of the Liver. *Cell Biology International Reports* 6 (6): 625–28.
- Guguen-Guillouzo, Christiane, and Andre Guillouzo. 2010. General Review on in Vitro Hepatocyte Models and Their Applications. *Methods in Molecular Biology* (Clifton, N.J.) 640: 1–40.
- Imanari, H., H. Kuroda, and K. Tamura. 1981. Microfilaments around the Bile Canaliculi in Patients with Intrahepatic Cholestasis. *Gastroenterologia Japonica* 16 (2): 168–73.
- Jansen, P. L., S. S. Strautnieks, E. Jacquemin, M. Hadchouel, E. M. Sokal, G. J. Hooiveld, J. H. Koning, et al. 1999. Hepatocanalicular Bile Salt Export Pump Deficiency in Patients with Progressive Familial Intrahepatic Cholestasis. *Gastroenterology* 117 (6): 1370–79.
- Jemnitz, Katalin, Zsuzsa Veres, Regina Tugyi, and Laszlo Vereczkey. 2010. Biliary Efflux Transporters Involved in the Clearance of Rosuvastatin in Sandwich Culture of Primary Rat Hepatocytes. *Toxicology in Vitro: An International Journal Published in Association with BIBRA* 24 (2): 605–10.

DMD # 71373

- Kaimal, Rajani, Xiulong Song, Bingfang Yan, Roberta King, and Ruitang Deng. 2009. Differential Modulation of Farnesoid X Receptor Signaling Pathway by the Thiazolidinediones. *The Journal of Pharmacology and Experimental Therapeutics* 330 (1): 125–34.
- Keisu, M., and T. B. Andersson. 2010. Drug-Induced Liver Injury in Humans: The Case of Ximelagatran. *Handbook of Experimental Pharmacology*, no. 196: 407–18.
- Kenna, J. Gerry. 2014. Current Concepts in Drug-Induced Bile Salt Export Pump (BSEP) Interference. *Current Protocols in Toxicology*. 61: 23.7.
- Kenne, Kerstin, Inger Skanberg, Bjorn Glinghammar, Alain Berson, Dominique Pessayre, Jean-Pierre Flinois, Philippe Beaune, et al. 2008. Prediction of Drug-Induced Liver Injury in Humans by Using in Vitro Methods: The Case of Ximelagatran. *Toxicology in Vitro: An International Journal Published in Association with BIBRA* 22 (3): 730–46.
- Köck, Kathleen, Brian C. Ferslew, Ida Netterberg, Kyunghee Yang, Thomas J. Urban, Peter W. Swaan, Paul W. Stewart, and Kim L. R. Brouwer. 2014. Risk Factors for Development of Cholestatic Drug-Induced Liver Injury: Inhibition of Hepatic Basolateral Bile Acid Transporters Multidrug Resistance-Associated Proteins 3 and 4. *Drug Metabolism and Disposition: The Biological Fate of Chemicals* 42 (4): 665–74.
- Kostrubsky, Seva E., Stephen C. Strom, Amit S. Kalgutkar, Shaila Kulkarni, James Atherton, Rouchelle Mireles, Bo Feng, et al. 2006. Inhibition of Hepatobiliary Transport as a Predictive Method for Clinical Hepatotoxicity of Nefazodone. *Toxicological Sciences: An Official Journal of the Society of Toxicology* 90 (2): 451–59.
- Lee, William M. 2003. Drug-Induced Hepatotoxicity. *The New England Journal of Medicine* 349 (5): 474–85.
- Liguori, Michael J., Eric A. G. Blomme, and Jeffrey F. Waring. 2008. Trovafloxacin-Induced Gene Expression Changes in Liver-Derived in Vitro Systems: Comparison of Primary Human Hepatocytes to HepG2 Cells. *Drug Metabolism and Disposition* 36 (2): 223–33.

DMD # 71373

Livertox (<http://livertox.nih.gov/>)

Longo, Dm, Y Yang, Pb Watkins, Ba Howell, and Sq Siler. 2016. Elucidating Differences in the Hepatotoxic Potential of Tolcapone and Entacapone With DILIsym®, a Mechanistic Model of Drug-Induced Liver Injury. *CPT: Pharmacometrics & Systems Pharmacology* 5 (1): 31–39.

Mano, Yuji, Takashi Usui, and Hidetaka Kamimura. 2007. Effects of Bosentan, an Endothelin Receptor Antagonist, on Bile Salt Export Pump and Multidrug Resistance–associated Protein 2. *Biopharmaceutics & Drug Disposition* 28 (1): 13–18.

May, Louis D., Jay H. Lefkowitz, Michael T. Kram, and David E. Rubin. 2002. Mixed Hepatocellular-Cholestatic Liver Injury after Pioglitazone Therapy. *Annals of Internal Medicine* 136 (6): 449–52.

McGill, Mitchell R., Matthew R. Sharpe, C. David Williams, Mohammad Taha, Steven C. Curry, and Hartmut Jaeschke. 2012. The Mechanism Underlying Acetaminophen-Induced Hepatotoxicity in Humans and Mice Involves Mitochondrial Damage and Nuclear DNA Fragmentation. *The Journal of Clinical Investigation* 122 (4): 1574–83.

Mihatsch, M. J., M. Kyo, K. Morozumi, Y. Yamaguchi, V. Nickeleit, and B. Ryffel. 1998. The Side-Effects of Ciclosporine-A and Tacrolimus. *Clinical Nephrology* 49 (6): 356–63.

Mohi-ud-din, Raja, and James H. Lewis. 2004. Drug- and Chemical-Induced Cholestasis. *Clinics in Liver Disease* 8 (1): 95–132.

Morgan, Ryan E., Michael Trauner, Carlo J. van Staden, Paul H. Lee, Bharath Ramachandran, Michael Eschenberg, Cynthia A. Afshari, Charles W. Qualls, Ruth Lightfoot-Dunn, and Hisham K. Hamadeh. 2010. Interference with Bile Salt Export Pump Function Is a Susceptibility Factor for Human Liver Injury in Drug Development. *Toxicological Sciences: An Official Journal of the Society of Toxicology* 118 (2): 485–500.

Morgan, Ryan E., Carlo J. van Staden, Yuan Chen, Natarajan Kalyanaraman, Jackson Kalanzi, Robert T. Dunn, Cynthia A. Afshari, and Hisham K. Hamadeh. 2013. A

DMD # 71373

- Multifactorial Approach to Hepatobiliary Transporter Assessment Enables Improved Therapeutic Compound Development. *Toxicological Sciences: An Official Journal of the Society of Toxicology* 136 (1): 216–41.
- Nammour, Fadel E., Nabil F. Fayad, and Steven R. Peikin. 2003. Metformin-Induced Cholestatic Hepatitis. *Endocrine Practice*: 9 (4): 307–9.
- Padda, Manmeet S., Mayra Sanchez, Abbasi J. Akhtar, and James L. Boyer. 2011. Drug-Induced Cholestasis. *Hepatology* 53 (4): 1377–87.
- Pauli-Magnus, Christiane, and Peter J. Meier. 2006. Hepatobiliary Transporters and Drug-Induced Cholestasis. *Hepatology* 44 (4): 778–87.
- Pedersen, Jenny M., Pär Matsson, Christel A. S. Bergström, Janet Hoogstraate, Agneta Norén, Edward L. LeCluyse, and Per Artursson. 2013. Early Identification of Clinically Relevant Drug Interactions with the Human Bile Salt Export Pump (BSEP/ABCB11). *Toxicological Sciences: An Official Journal of the Society of Toxicology* 136 (2): 328–43.
- Pomponio, Giuliana, Camille C. Savary, Céline Parmentier, Frederic Bois, André Guillouzo, Luca Romanelli, Lysiane Richert, Emma Di Consiglio, and Emanuela Testai. 2015. In Vitro Kinetics of Amiodarone and Its Major Metabolite in Two Human Liver Cell Models after Acute and Repeated Treatments. *Toxicology in Vitro, The Predict-IV project: Towards predictive toxicology using in vitro techniques*, 30 (1, Part A): 36–51.
- Regenthal, R., M. Krueger, C. Koepfel, and R. Preiss. 1999. Drug Levels: Therapeutic and Toxic Serum/plasma Concentrations of Common Drugs. *Journal of Clinical Monitoring and Computing* 15 (7-8): 529–44.
- Saadi, Tarek, Matti Waterman, Heba Yassin, and Yaacov Baruch. 2013. Metformin-Induced Mixed Hepatocellular and Cholestatic Hepatic Injury: Case Report and Literature Review. *International Journal of General Medicine* 6 (August): 703–6.
- Schadt, S., S. Simon, S. Kustermann, F. Boess, C. McGinnis, A. Brink, R. Lieven, et al. 2015. Minimizing DILI Risk in Drug Discovery - A Screening Tool for Drug

DMD # 71373

- Candidates. *Toxicology in Vitro: An International Journal Published in Association with BIBRA 30 (1 Pt B)*: 429–37.
- Sharanek, Ahmad, Pamela Bachour-El Azzi, Houssein Al-Attrache, Camille C. Savary, Lydie Humbert, Dominique Rainteau, Christiane Guguen-Guillouzo, and André Guillouzo. 2014. Different Dose-Dependent Mechanisms Are Involved in Early Cyclosporine a-Induced Cholestatic Effects in hepaRG Cells. *Toxicological Sciences: An Official Journal of the Society of Toxicology* 141 (1): 244–53.
- Sharanek, Ahmad, Audrey Burban, Lydie Humbert, Pamela Bachour-El Azzi, Neuza Felix-Gomes, Dominique Rainteau, and Andre Guillouzo. 2015. Cellular Accumulation and Toxic Effects of Bile Acids in Cyclosporine A-Treated HepaRG Hepatocytes. *Toxicological Sciences: An Official Journal of the Society of Toxicology* 147 (2): 573–87.
- Sharanek, Ahmad, Audrey Burban, Matthew Burbank, Rémy Le Guevel, Ruoya Li, André Guillouzo, and Christiane Guguen-Guillouzo. 2016. Rho-Kinase/myosin Light Chain Kinase Pathway Plays a Key Role in the Impairment of Bile Canaliculi Dynamics Induced by Cholestatic Drugs. *Scientific Reports* 6 (May): 24709.
- Smith, Kirsten S., Philip L. Smith, Tiffany N. Heady, Joel M. Trugman, W. Dean Harman, and Timothy L. Macdonald. 2003. In Vitro Metabolism of Tolcapone to Reactive Intermediates: Relevance to Tolcapone Liver Toxicity. *Chemical Research in Toxicology* 16 (2): 123–28.
- Spigset, Olav, Staffan Hägg, and Andrew Bate. 2003. Hepatic Injury and Pancreatitis during Treatment with Serotonin Reuptake Inhibitors: Data from the World Health Organization (WHO) Database of Adverse Drug Reactions. *International Clinical Psychopharmacology* 18 (3): 157–61.
- Stieger, Bruno. 2010. Role of the Bile Salt Export Pump, BSEP, in Acquired Forms of Cholestasis. *Drug Metabolism Reviews* 42 (3): 437–45.

DMD # 71373

- Swift*, Brandon, Nathan D. Pfeifer*, and Kim L.R. Brouwer. 2010. Sandwich-Cultured Hepatocytes: An in Vitro Model to Evaluate Hepatobiliary Transporter-Based Drug Interactions and Hepatotoxicity. *Drug Metabolism Reviews* 42 (3): 446–71.
- Thibault, N., J. R. Claude, and F. Ballet. 1992. Actin Filament Alteration as a Potential Marker for Cholestasis: A Study in Isolated Rat Hepatocyte Couplets. *Toxicology* 73 (3): 269–79.
- Toyoda, Yu, Miho Tamai, Kasumi Kashikura, Shunsuke Kobayashi, Yoichi Fujiyama, Tomoyoshi Soga, and Yoh-ichi Tagawa. 2012. Acetaminophen-Induced Hepatotoxicity in a Liver Tissue Model Consisting of Primary Hepatocytes Assembling around an Endothelial Cell Network. *Drug Metabolism and Disposition: The Biological Fate of Chemicals* 40 (1): 169–77.
- Treiber, A., R. Schneiter, S. Hausler, and B. Stieger. 2007. Bosentan Is a Substrate of Human OATP1B1 and OATP1B3: Inhibition of Hepatic Uptake as the Common Mechanism of Its Interactions with Cyclosporin A, Rifampicin, and Sildenafil. *Drug Metabolism and Disposition* 35 (8): 1400–1407.
- Tujios, Shannan, and Robert J. Fontana. 2011. Mechanisms of Drug-Induced Liver Injury: From Bedside to Bench. *Nature Reviews. Gastroenterology & Hepatology* 8 (4): 202–11.
- Velayudham, Lakshumanan S., and Geoffrey C. Farrell. 2003. Drug-Induced Cholestasis. *Expert Opinion on Drug Safety* 2 (3): 287–304.
- Watanabe, Norihito, Nobuhiro Tsukada, Charles R. Smith, and M. James Phillips. 1991. Motility of Bile Canaliculi in the Living Animal: Implications for Bile Flow. *The Journal of Cell Biology* 113 (5): 1069–80.
- Watkins Paul B., Randall W. Whitcomb. 1998. Hepatic Dysfunction Associated with Troglitazone. *The New England Journal of Medicine* 338 (13): 916–17.
- Xu, Jinghai J., Peter V. Henstock, Margaret C. Dunn, Arthur R. Smith, Jeffrey R. Chabot, and David de Graaf. 2008. Cellular Imaging Predictions of Clinical Drug-Induced Liver

DMD # 71373

- Injury. *Toxicological Sciences: An Official Journal of the Society of Toxicology* 105 (1): 97–105.
- Zamek-Gliszczyński, M. J., K. A. Hoffmaster, D. J. Tweedie, K. M. Giacomini, and K. M. Hillgren. 2012. Highlights from the International Transporter Consortium Second Workshop. *Clinical Pharmacology and Therapeutics* 92 (5): 553–56.
- Zollner, G., P. Fickert, R. Zenz, A. Fuchsbichler, C. Stumptner, L. Kenner, P. Ferenci, et al. 2001. Hepatobiliary Transporter Expression in Percutaneous Liver Biopsies of Patients with Cholestatic Liver Diseases. *Hepatology (Baltimore, Md.)* 33 (3): 633–46.

DMD # 71373

Footnotes

Financial support

This work was supported by the European Community [Contract MIP-DILI-115336]. The MIP-DILI project has received support from the Innovative Medicines Initiative Joint Undertaking, resources of which are composed of financial contribution from the European Union's Seventh Framework Programme [FP7/20072013] and EFPIA companies' in kind contribution. <http://www.imi.europa.eu/>.

Matthew G. Burbank was financially supported by a CIFRE PhD contract with Servier, and Audrey Burban and Ahmad Sharanek by the MIP-DILI project.

Address reprint requests to: Prof. André Guillouzo, INSERM U991, Faculté de Pharmacie. 2 avenue L. Bernard, 35043 Rennes cedex, France. E-mail address : andre.guillouzo@univ-rennes1.fr

DMD # 71373

Legends to Figures

Fig. 1. Effect of cholestatic and non cholestatic drugs on bile canaliculi dynamics in HepaRG cells

(A, B) Phase-contrast images after 2h-treatment showing dilatation (red arrows), constriction (green arrows) or no change (yellow arrows), (bar =50 μ m). (C) CsA 10 μ M effects after 3h. (D) Tolcapone (TOL) effects after 1 and 6h. (E) Negative compounds (XIM and AMI) effects after 2h. (F, G, H, I). BC surfaces of HepaRG cells exposed to dilatators, constrictors, tolcapone/entacapone and control compounds were quantified. Briefly, BC surface quantification was based on brightness parameters that were adjusted to eliminate non corresponding objects and analysis was performed on at least 3 different experiments. White canalicular lumen was then quantified using image J software every 10min for 24h. AMI, amiodarone; APAP, acetaminophen; BOS, bosentan; BUS, buspirone; CIM, cimetidine; CPZ, chlorpromazine; CsA, cyclosporine A; DIC, diclofenac; ENT, entacapone; FIA, fialuridine; MET, metformin; NEF, nefazodone; PER, perhexiline; PIO, pioglitazone; TAC, tacrolimus; TOL, tolcapone; TRO, troglitazone; XIM, ximelagatran. Data were expressed relative to untreated cells, arbitrarily set at a value of 100%. Data represent the means \pm SEM of three independent experiments. All dilatators showed at least transiently enlarged BC >125%.

Fig. 2. Alterations of MLC2 phosphorylation/dephosphorylation by cholestatic drugs in HepaRG cells.

(A) Representative western blots of p-MLC2 in comparison with HSC70 using anti-S19 phospho MLC2 and anti-HSC70 antibodies, at various time points (1, 2 and 3h) in cells treated with groups 1 and 2 cholestatic drugs. (B, D) Graphical representation of MLC2

DMD # 71373

phosphorylation/dephosphorylation quantified using fusion-CAPT software. **(C)** Western blots of p-MLC2 obtained with group 3 molecules. AMI, amiodarone; APAP, acetaminophen; BOS, bosentan; BUS, buspirone; CIM, cimetidine; CPZ, chlorpromazine; CsA, cyclosporine A; DIC, diclofenac; ENT, entacapone; FIA, fialuridine; MET, metformin; NEF, nefazodone; PER, perhexiline; PIO, pioglitazone; TAC, tacrolimus; TOL, tolcapone; TRO, troglitazone; XIM, ximelagatran. Data are expressed in arbitrary units (A.U) and represent means \pm SEM of 3 independent experiments. One hour treatment was arbitrarily set at a fixed value of 2.5 for all the drugs. Data were considered significantly different when $*P < 0.05$.

Fig. 3. Alterations of the ROCK/MLCK pathway by cholestatic drugs in HepaRG cells.

(A) BC surface quantification following Y-27632 (10 μ M) and CaM (5 μ M) treatments for 4h. **(B)** Cells treated with 200 μ M DIC +/- the MLCK activator CaM (5 μ M) for 2h. Phase-contrast images (bar = 50 μ m). **(C)** Cells treated with 75 μ M NEF +/- the ROCK inhibitor Y-27632 (10 μ M) for 2h. Phase-contrast images (bar = 50 μ m). BC surface quantification with constrictors as described above **(D)**, tolcapone and entacapone **(E)** and dilators **(F)**. **(G)** Cells treated with 100 μ M BOS +/- Y-27632 (10 μ M) or Y-27632 (10 μ M) alone for 2h. Phase-contrast images (bar = 50 μ m). Data are expressed relative to untreated cells, arbitrarily set at a value of 100%. Data represent the means \pm SEM of three independent experiments. Data were considered significantly different when $^{\#}P < 0.001$.

Fig. 4. Effects of tested drugs on bile acid clearance activity in HepaRG cells

[3 H]-TCA clearance in HepaRG cells treated with group 1 **(A)**, group 2 **(B)** and group 3 **(C)** drugs for 2h. [3 H]-TCA clearance was determined based on its accumulation in cell layers

DMD # 71373

(Ctrl = control). Data were expressed relative to the levels found in untreated cells, arbitrarily set at a value of 100%. Data represent the means \pm SEM of three independent experiments * $P < 0.05$, ** $P < 0.01$ and *** $P < 0.001$ compared with untreated cells.

Fig. 5. Disruption of bile canaliculi rhythmic movements in 4-day primary human hepatocyte cultures.

(A, B) Phase-contrast images (bar = 50 μ m) after 2h-treatment showing untreated cells (control) and cells treated with constrictors (i.e. 50 μ M CPZ; 50 μ M CsA; 75 μ M NEF; 100 μ M TRO), with 100 μ M TOL or with dilators (100 μ M ENT, 200 μ M DIC and 100 μ M BOS). **(C)** Results obtained with hepatocytes from the 3 donors treated with different drugs. CPZ, chlorpromazine; CsA, cyclosporine A; NEF, nefazodone; TRO, troglitazone; TOL, tolcapone; BOS, bosentan; ENT, entacapone; DIC, diclofenac; BOS, bosentan; PER, perhexiline; FIA, fialuridine. nc: no change.

Fig. 6. Schematic representation of the molecular targets of cholestatic drugs.

(A) Dilators and tolcapone (within the first hour) inhibit Ca^{2+} /CaM-dependent MLCK leading to dilatation. **(B)** Constrictors and tolcapone (after 1h) activate ROCK activity and maintain abnormal high MLC2, thereby leading to BC constriction. Y-27632 inhibits ROCK activity and causes MLC2 dephosphorylation, thereby leading to BC dilatation. ROCK, Rho-kinase; Ca^{2+} , calcium; CaM, calmodulin; MLCK, myosin light chain kinase.

DMD # 71373

Table 1. Characteristics of the 18 tested drugs.

The list of compounds, their therapeutic use, clinical hepatic effects and some results obtained in *in vitro* with either vesicles overexpressing human BA transporters (*) or liver cells (**) are displayed. These compounds include the 14 training compounds of the MIP-DILI project plus chlorpromazine, cyclosporine A, tacrolimus and cimetidine. Compounds were classified into 3 groups based on their reported cholestatic potential in clinic: Group 1: drugs involved in clinical cholestasis; group 2: drugs involved in rare cases of clinical cholestasis and group 3: drugs not involved in clinical cholestasis. AMI, amiodarone; APAP, acetaminophen; BOS, bosentan; BUS, buspirone; CIM, cimetidine; CPZ, chlorpromazine; CsA, cyclosporine A; DIC, diclofenac; ENT, entacapone; FIA, fialuridine; MET, metformin; NEF, nefazodone; PER, perhexiline; PIO, pioglitazone; TAC, tacrolimus; TOL, tolcapone; TRO, troglitazone; XIM, ximelagatran.

	Drugs	Therapeutic use	Clinical hepatic effects	<i>In vitro</i> hepatic effects	Main references
Group 1. DRUGS involved in clinical cholestasis	BOS	Antihypertensive	Aminotransferases elevation ; increase in serum bile acids	BSEP inhibition* ; substrate for OATP, NTCP and MRP2**	Fattinger et al. 2001 ; Mano et al. 2007 ; Treiber et al. 2007 ; Livertox
	CPZ	Antipsychotic	Intrahepatic cholestasis ; hepatocellular necrosis ; phospholipidosis	Oxidative stress ; mitochondrial membrane potential loss ; pericanalicular F-actin disorganisation	Anthérieu et al. 2013 ; Padda et al. 2011 ; Velayudham and Farell 2003 ; Livertox
	CsA	Immunosup- pressant	Cholestasis; hyperbilirubinemia ; Aminotransferases elevation	Oxidative stress ; BSEP, MRP2 and MDR1 inhibition** ; bile acid transport alteration ; pericanalicular F-actin disorganisation	Sharanek et al. 2015 ; Mihatsch et al. 1998

DMD # 71373

Group 2. DRUGS involved in rare cases of clinical cholestasis	NEF	Antidepressant	Cholestatic hepatitis ; hepatocellular necrosis	Inhibition of mitochondrial respiration ; BSEP inhibition*	Spigset et al. 2003 ; Dykens et al. 2008 ; Kostrubsky et al. 2006 ; Morgan et al. 2010 ; Livertox
	TRO	Antidiabetic	Serious idiosyncratic liver injury ; hepatocyte necrosis ; cholestatic hepatitis	Bile acid transporters inhibition ; mitochondrial dysfunction ; BSEP inhibition*	Watkins et al. 1998 ; Jemnitz et al. 2010 ; Morgan et al. 2010 ; Livertox
	CIM	Histamine2- receptor antagonist	Hepatocellular-cholestatic injury	BSEP inhibition*	Livertox ; Mohi-ud- din et al. 2004 ; Pedersen et al. 2013
	DIC	AINS	Cholestasis ; aminotransferases elevation	BSEP inhibition* ; BSEP and MRP2 inhibition**	Banks et al. 1995 ; Livertox ; Pedersen et al. 2013
	ENT	Antiparkinsonian	Mild jaundice and cholestatic pattern ; aminotransferases elevation	BSEP and NTCP inhibition* ; mitochondrial dysfunction	Fisher et al. 2002 ; Longo et al. 2016 ; Livertox ; Krajcsi P. (Solvo, HU) unpublished data
	MET	Antidiabetic	Cholestatic hepatitis ; mixed hepatocellular and cholestatic injury	Bile acid accumulation ; liver mitochondria injury ; BSEP inhibition*	Nammour et al. 2003 ; Saadi et al. 2013 ; Livertox ; Krajcsi P. (Solvo, HU) unpublished data
	PER	Prophylactic antianginal	Steatohepatitis ; rare cases of cholestasis	ROS formation ; lipid peroxidation ; BSEP and NTCP inhibition*	Feuer et al. 1992 ; Krajcsi P. (Solvo, HU) unpublished data
	TAC	Immunosuppressant	Cholestasis after transplantation (Infant) ; moderate aminotransferases elevation	BSEP inhibition* ; <i>BSEP and NTCP inhibition**</i> ; BSEP internalization**	Sharanek et al. 2014 ; Mihatsch et al. 1998 ; Livertox
	TOL	Antiparkinsonian	Aminotransferases elevation ; intrahepatic cholestasis	ROS formation ; mitochondrial toxicity ; NTCP, BSEP, MRP2, MRP3 and MRP4 inhibition* ;	Smith et al. 2003 ; Morgan et al. 2013 ; Krajcsi P. (Solvo,

DMD # 71373

				reactive metabolite	HU) unpublished data ; Longo et al. 2016
Group 3. DRUGS not involved in clinical cholestasis	AMI	Antiarrhythmic	Steatosis ; phospholipidosis ; aminotransferases elevation	Phospholipidosis ; steatosis	Fromenty et al. 1995 ; Anthérieu et al. 2011
	APAP	Analgesic and antipyretic	Acute liver failure ; aminotransferases elevation	Lactate dehydrogenase increase ; mitochondrial damage	Toyoda et al. 2012 ; McGill et al. 2012
	BUS	Hypnotic	Rare aminotransferase elevation with no link to clinically apparent liver injury	No inhibition of mitochondrial respiration	Kostrubsky et al. 2006 ; Dykens et al. 2008 ; Livertox
	FIA	Antiviral	Liver failure associated with lactic acidosis ; mitochondrial toxicity	Mitochondrial and cellular toxicity	Tujios S et al. 2011
	PIO	Antidiabetic (PPAR-γ agonist)	No aminotransferase elevation	MRP2 stimulation ; BSEP and MRP4 inhibition*	Morgan et al. 2010 ; Livertox
	XIM	Anticoagulant	Immune toxicity: aminotransferase elevation	No formation of reactive metabolites	Keisu et al. 2010 ; Kenne et al. 2008

DMD # 71373

Table 2. Cmax, IC20 and maximum tested concentrations of the 18 tested drugs

Cmax values are from the literature (Regenthal et al. 1999; Chu et al. 2007; Xu et al. 2008; Dhillon and Keating 2009; Keisu and Andersson 2010; Dawson et al. 2012; Sharanek et al. 2014; Schadt et al. 2015). Cells were incubated for 24h with different concentrations of each drug. For cytotoxicity testing the cells were treated with varying concentrations of each drug for 24h, then assayed with the MTT colorimetric test and IC20s values were calculated. Cmax refers to the maximum serum concentration of the drug (μM). Drug abbreviations as in Table 1.

	Drugs	Cmax (μM)	IC20 (μM) (24h)	Maximun <i>in vitro</i> concentration tested (μM)
Group 1. DRUGS involved in clinical cholestasis	BOS	7.4	120	100
	CPZ	0.2	50	50
	CsA	1.15	-	50
	NEF	4.26	50	75
	TRO	6.39	65	50
Group 2. DRUGS involved in rare cases of clinical cholestasis	CIM	4.9	4000	4000
	DIC	8	375	200
	ENT	3.9	250	100
	MET	7.74	3000	3000
	PER	2	25	20
	TAC	0.09	60	50
	TOL	23	70	100
Group 3. DRUGS not involved in clinical cholestasis	AMI	0.8	20	20
	APAP	139	20000	25000
	BUS	0.01	>300	100
	FIA	0.64	>300	100
	PIO	4.2	200	100
	XIM	0.3	>300	100

DMD # 71373

Table 3. Effects of drugs tested on transcript levels of different hepatic transporters.

HepaRG cells were exposed to the 3 groups of compounds at the indicated concentration for 24h. mRNA levels were measured by RT-PCR analysis. All results are expressed relative to the levels found in control cells, arbitrarily set at a value of 1. * $P < 0.05$, ** $P < 0.01$ and *** $P < 0.001$ compared with untreated cells.

Drugs		Bile acids transporters					
		<i>BSEP</i>	<i>NTCP</i>	<i>OATB-B</i>	<i>MRP2</i>	<i>MRP3</i>	<i>MRP4</i>
Group 1. DRUGS involved in clinical cholestasis	Bosentan (100µM)	0.10 ± 0.01***	0.23 ± 0.06***	0.40 ± 0.02*	0.99 ± 0.16	0.62 ± 0.08	1.08 ± 0.16
	Chlorpromazine (50µM)	0.5 ± 0.2*	0.5 ± 0.1*	1.1 ± 0.1	1.2 ± 0.2	0.8 ± 0.2	1.7 ± 0.2*
	Cyclosporine (50µM)	0.54 ± 0.15**	0.05 ± 0.01***	0.17 ± 0.02***	1.8 ± 0.15***	1.79 ± 0.08***	2.68 ± 0.12***
	Nefazodone (75µM)	0.28 ± 0.08*	0.16 ± 0.06***	0.32 ± 0.07***	1.00 ± 0.1	0.90 ± 0.12	1.40 ± 0.2
	Troglitazone (50µM)	0.58 ± 0.11*	0.51 ± 0.06*	0.89 ± 0.14	0.88 ± 0.08	1.11 ± 0.10	0.86 ± 0.09
Group 2. DRUGS involved in rare cases of clinical cholestasis	Cimetidine (4mM)	0.33 ± 0.04***	0.21 ± 0.05**	0.63 ± 0.09	1.00 ± 0.31	0.89 ± 0.07	0.99 ± 0.26
	Diclofenac (200µM)	0.66 ± 0.1*	0.56 ± 0.1**	0.7 ± 0.06**	1.67 ± 0.09***	0.75 ± 0.06	0.74 ± 0.02**
	Entacapone (100µM)	0.83 ± 0.18	1.48 ± 0.12	1.13 ± 0.18	0.93 ± 0.11	0.98 ± 0.18	1.28 ± 0.08
	Metformin (3mM)	0.30 ± 0.06***	0.15 ± 0.04**	0.37 ± 0.14*	1.11 ± 0.16	1.00 ± 0.15	1.05 ± 0.26
	Perhexiline (20µM)	0.45 ± 0.09*	0.38 ± 0.07***	0.63 ± 0.11	0.96 ± 0.13	0.52 ± 0.06**	1.43 ± 0.15
	Tacrolimus (50µM)	0.44 ± 0.11**	0.23 ± 0.08***	0.43 ± 0.19*	2.04 ± 0.41*	1.64 ± 0.32*	2.60 ± 0.51*
	Tolcapone	0.20 ± 0.04***	0.25 ± 0.11***	0.27 ± 0.13***	0.56 ± 0.06**	0.48 ± 0.05*	1.19 ± 0.28

DMD # 71373

		(100µM)					
Group 3. DRUGS not involved in clinical cholestasis	Amiodarone (20µM)	1.34 ± 0.19	0.44 ± 0.09*	0.82 ± 0.05	0.90 ± 0.07	0.66 ± 0.07	1.35 ± 0.24
	APAP (25mM)	0.63 ± 0.14	0.53 ± 0.17	0.73 ± 0.03	0.69 ± 0.32	0.82 ± 0.20	1.31 ± 0.27
	Buspirone (100µM)	0.32 ± 0.03**	0.35 ± 0.12*	0.52 ± 0.15	1.20 ± 0.07	1.02 ± 0.06	1.67 ± 0.33
	Fialuridine (100µM)	0.66 ± 0.08	0.86 ± 0.1	0.97 ± 0.11	1.00 ± 0.06	0.97 ± 0.09	0.94 ± 0.07
	Pioglitazone (100µM)	0.66 ± 0.08*	0.31 ± 0.12*	0.59 ± 0.24	1.27 ± 0.29	1.03 ± 0.09	1.03 ± 0.10
	Ximelagatran (100µM)	1.19 ± 0.16	1.21 ± 0.20	1.14 ± 0.28	0.72 ± 0.09	0.92 ± 0.14	0.76 ± 0.10

DMD # 71373

Table 4. Summary of the results on the 18 tested drugs

BC deformation (i.e. constriction or dilatation), BSEP inhibition from the literature (vesicles), [³H]-TCA Clearance (control=100%), BSEP mRNA expression (control=1), MLC2 phosphorylation state and MLCK/ROCK implication are summarized. Human BSEP inhibition levels in transfected vesicles are taken from the literature: ^a(Pedersen et al. 2013) ^b(Morgan et al. 2010) ^c(Dawson et al. 2012) ^d(Krajcsi P, Solvo, HU; unpublished data) and expressed as high (++) , medium (+) and low or absent (-). BC, bile canaliculi; ROCK, Rho-kinase; MLCK, myosin light chain kinase; nc: no change. Drug abbreviations as in Table 1.

	Drugs	BC deformation	BSEP inhibition (vesicles)	[³ H]-TCA Clearance (ctrl = 100%)	BSEP mRNA expression (ctrl = 1)	MLC2 phosphorylation state	MLCK/ROCK implication
Group 1. DRUGS involved in clinical cholestasis	BOS	Dilatation	++ ^{a,b,c,d}	64.24 ± 4.13**	0.10 ± 0.01***	Dephosphorylation	MLCK
	CPZ	Constriction	+ ^{a,c,d}	49.96 ± 5.14*	0.5 ± 0.2*	Phosphorylation	ROCK
	CsA	Constriction	++ ^{a,b,c,d}	13.16 ± 1.48**	0.54 ± 0.15**	Phosphorylation	ROCK
	NEF	Constriction	++ ^{a,b,c,d}	52.46 ± 3.87***	0.28 ± 0.08*	Phosphorylation	ROCK
	TRO	Constriction	++ ^{a,b,c,d}	21.97 ± 3.72***	0.58 ± 0.11*	Phosphorylation	ROCK
Group 2. DRUGS involved in rare cases of clinical cholestasis	CIM	Dilatation	+ ^a	86.25 ± 12.12	0.33 ± 0.04***	Dephosphorylation	MLCK
	DIC	Dilatation	+ ^{a,d}	384.8 ± 57.96**	0.66 ± 0.1*	Dephosphorylation	MLCK
	ENT	Dilatation	- ^{b,d}	109.2 ± 16.94	0.83 ± 0.18	Dephosphorylation	MLCK
	MET	Constriction	- ^{a,d}	99.41 ± 8.45	0.30 ± 0.06***	Phosphorylation	ROCK
	PER	Constriction	- ^d	41.43 ± 8.22**	0.45 ± 0.09*	Phosphorylation	ROCK
	TAC	Dilatation	- ^b	56.14 ± 2.71***	0.44 ± 0.11**	Dephosphorylation	MLCK
	TOL	Dilatation then constriction	+ ^{b,c,d}	48.36 ± 8.14**	0.20 ± 0.04***	nc	MLCK - ROCK

DMD # 71373

Group 3. DRUGS not involved in clinical cholestasis	AMI	nc	+ ^{a,b,d}	115.6 ± 15.62	1.34 ± 0.19	nc	-
	APAP	nc	- ^{c,d}	137.2 ± 24.33	0.63 ± 0.14	nc	-
	BUS	nc	- ^{a,c,d}	86.07 ± 13.39	0.32 ± 0.03**	nc	-
	FIA	nc	- ^d	91.34 ± 9.14	0.66 ± 0.08	nc	-
	PIO	nc	+ ^{a,b,c,d}	86.15 ± 3.34	0.66 ± 0.08	nc	-
	XIM	nc	- ^d	96.71 ± 10.91	1.19 ± 0.16	nc	-

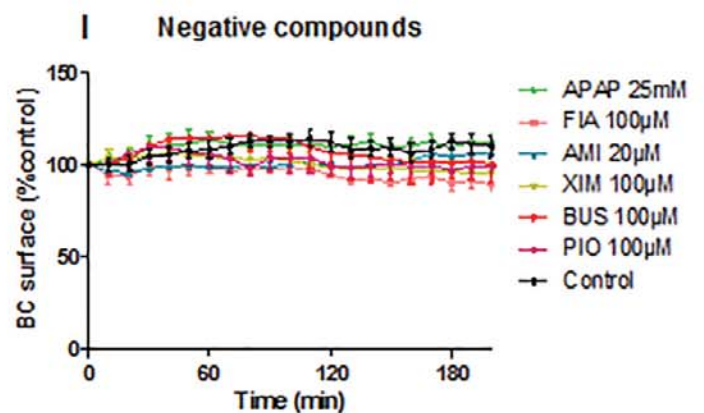
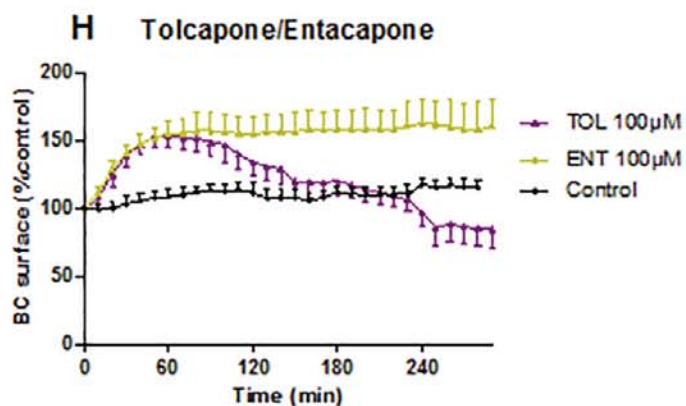
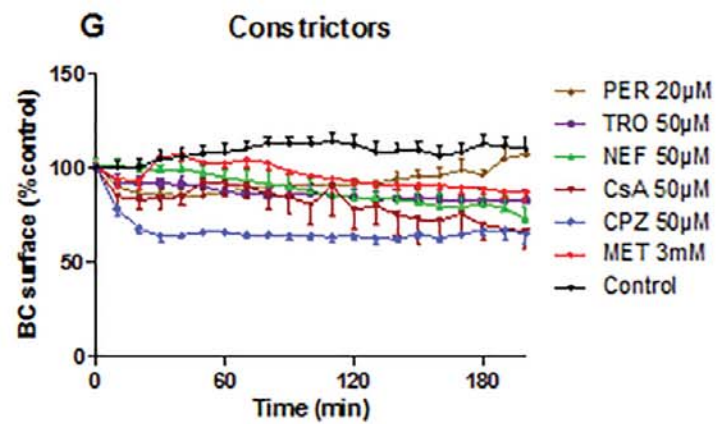
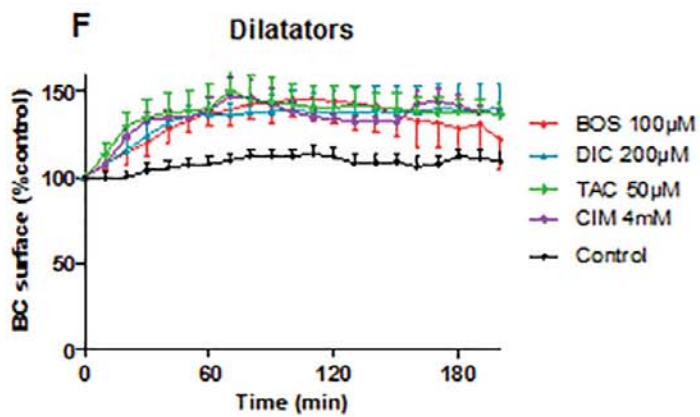
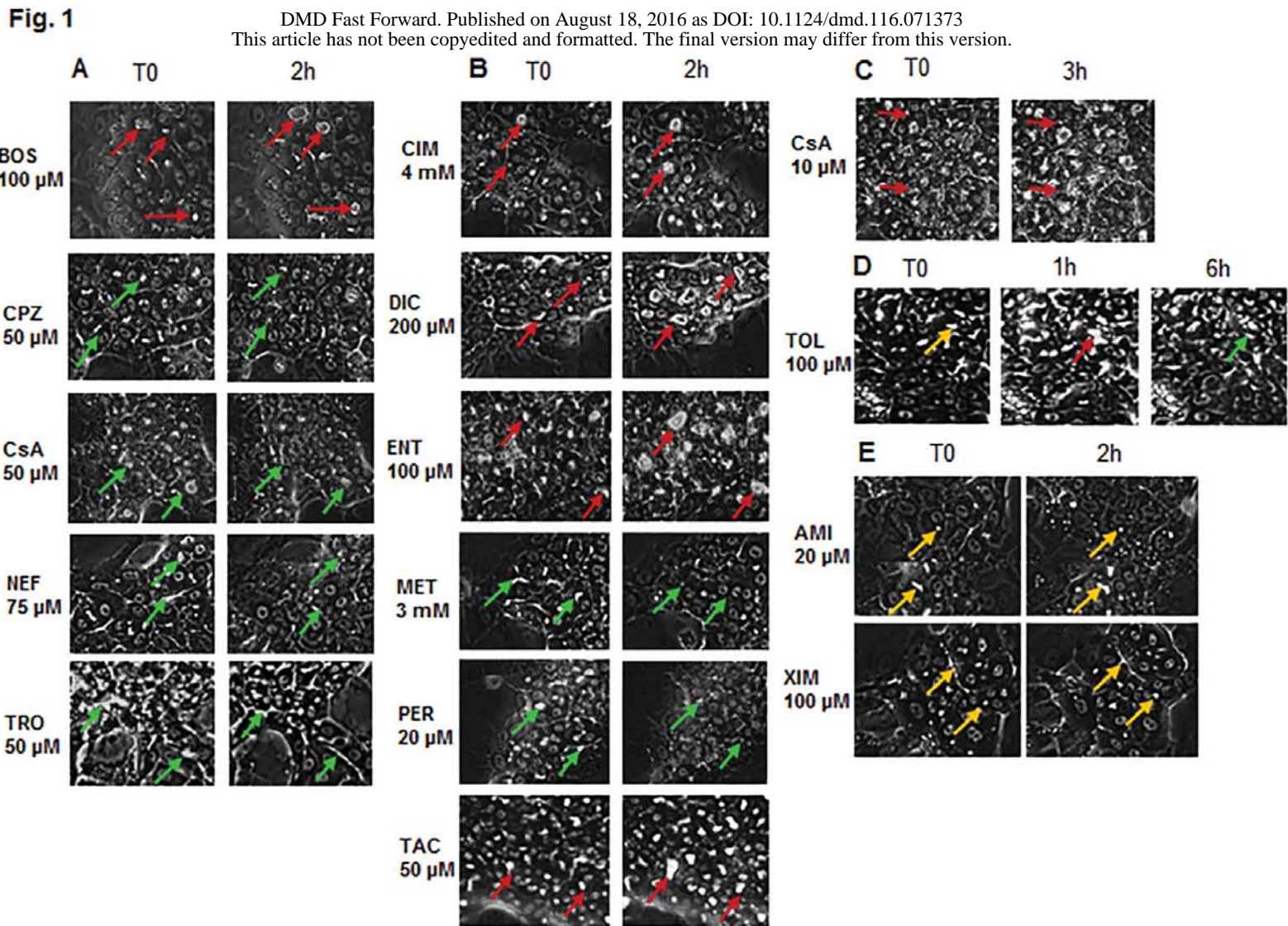
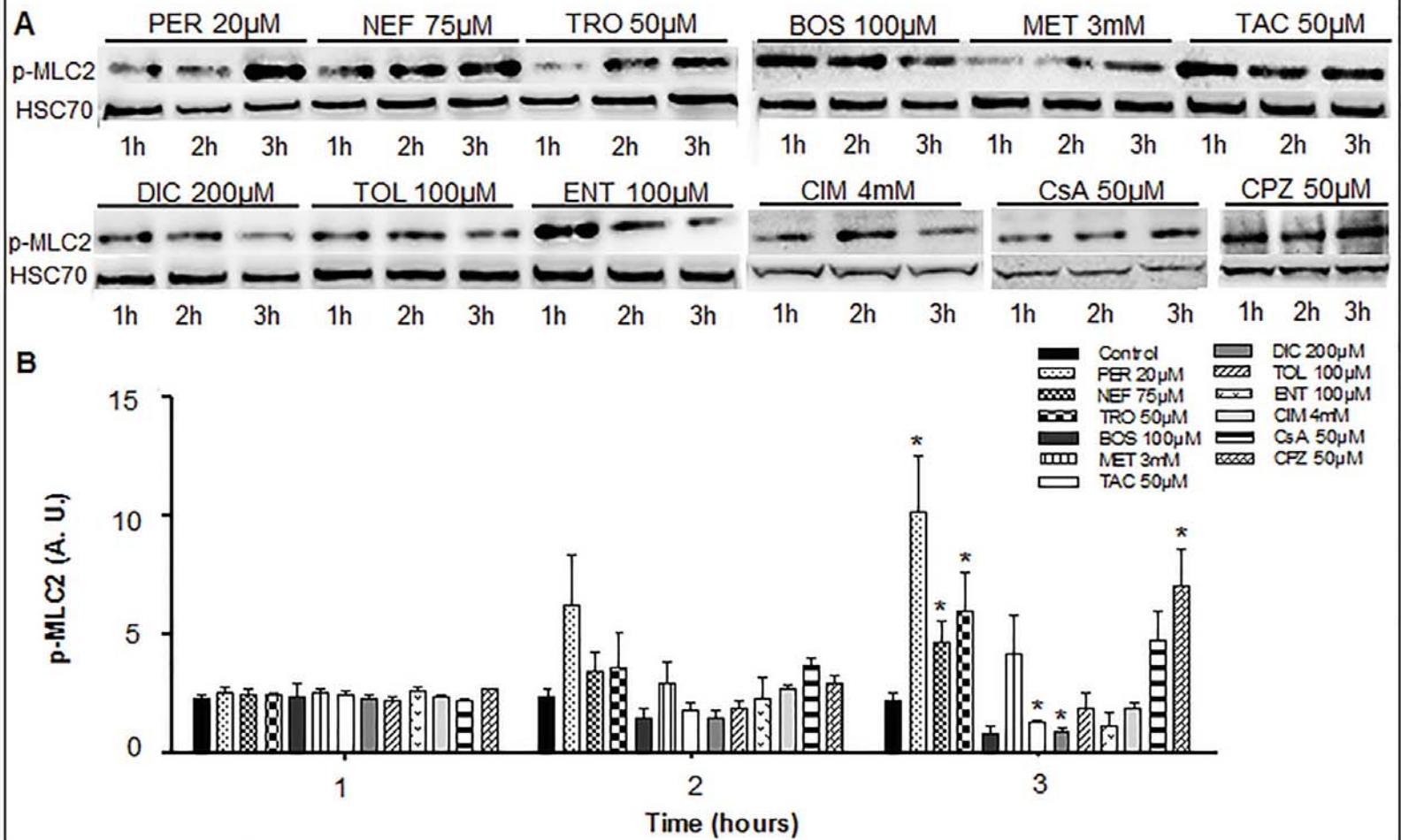


Fig. 2

Cholestatic drugs



Non cholestatic drugs

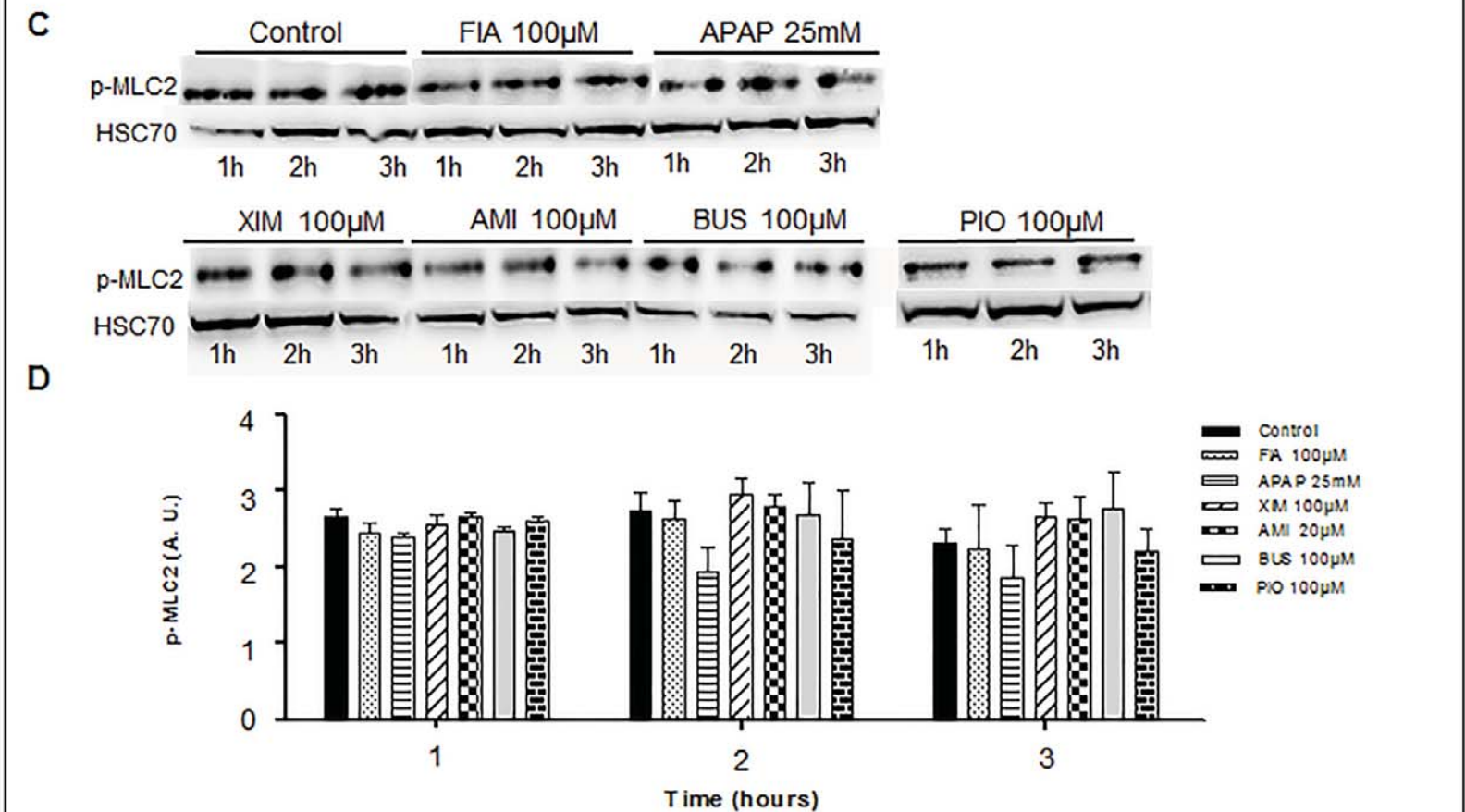
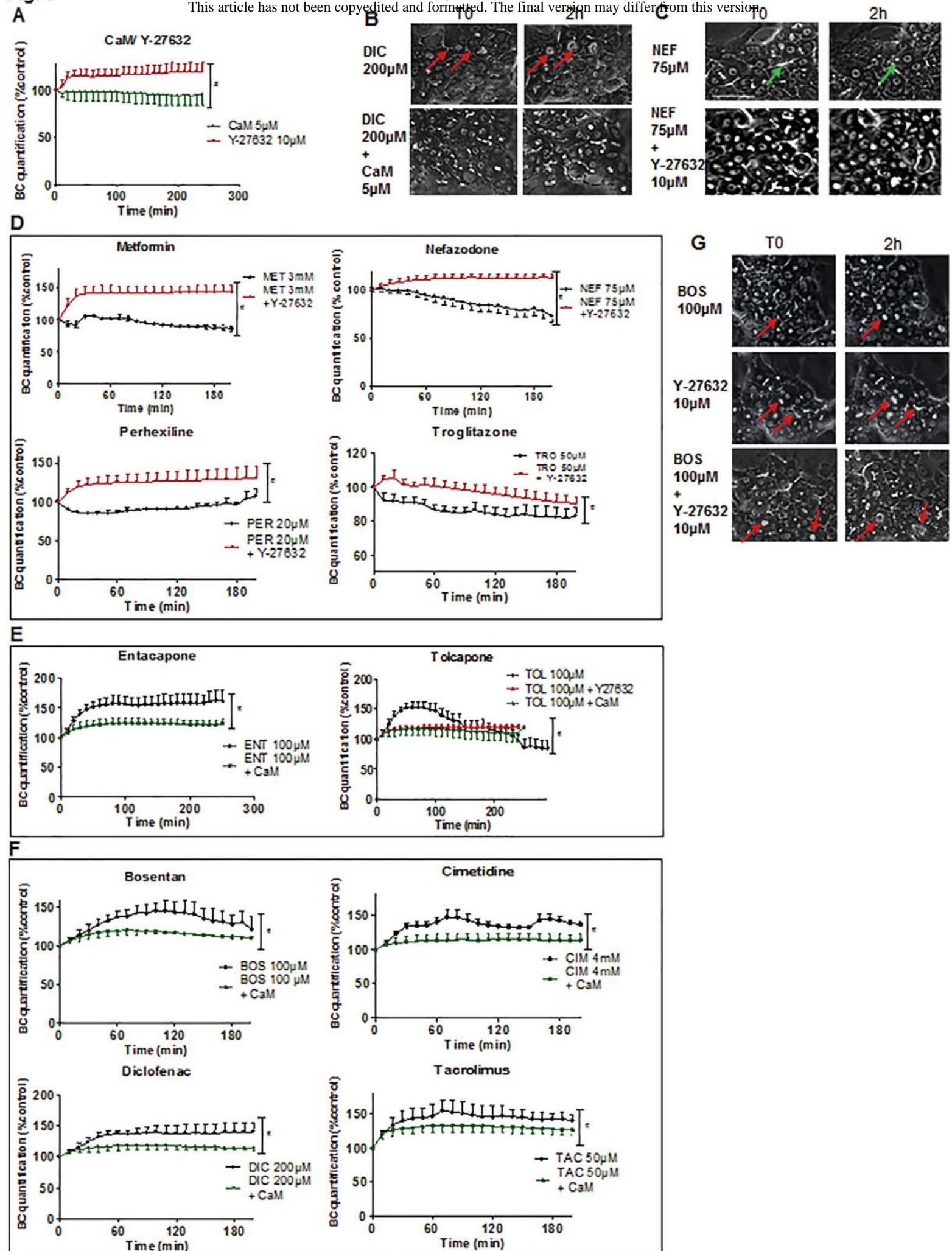
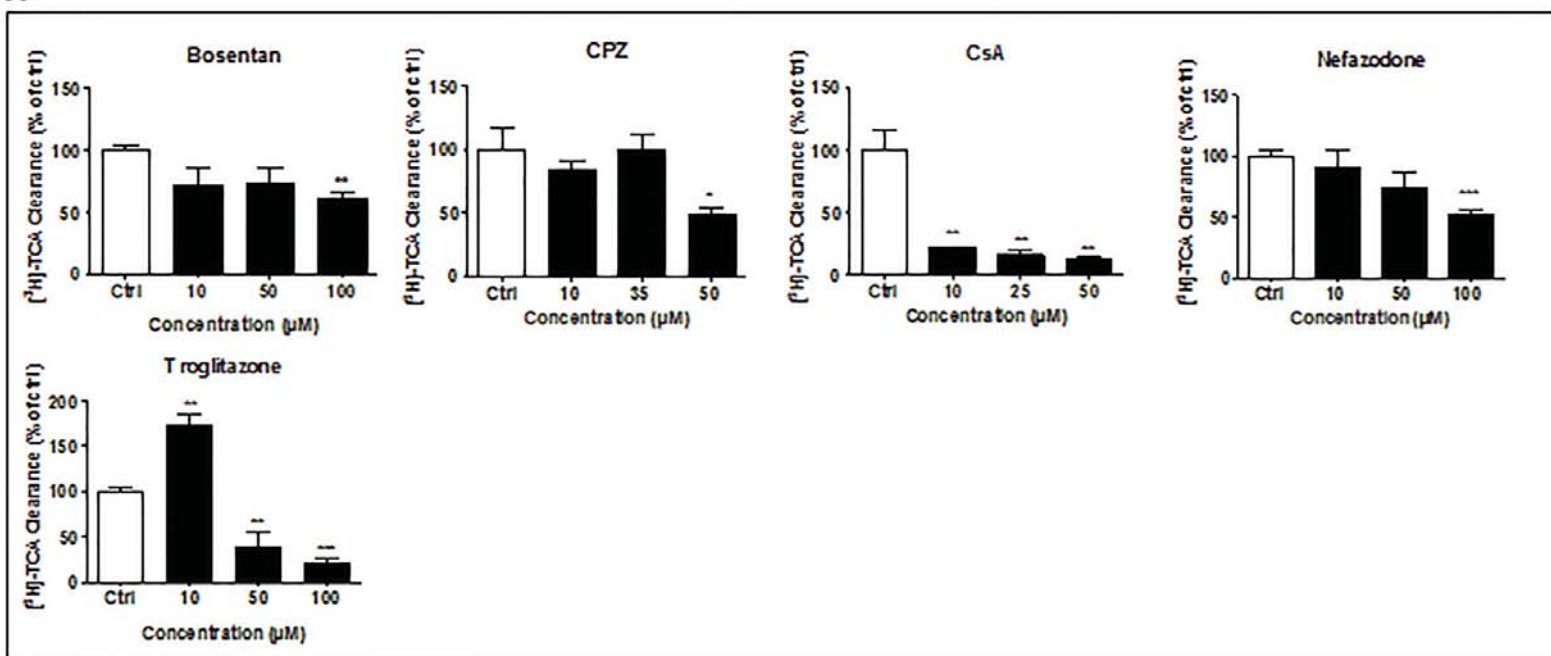


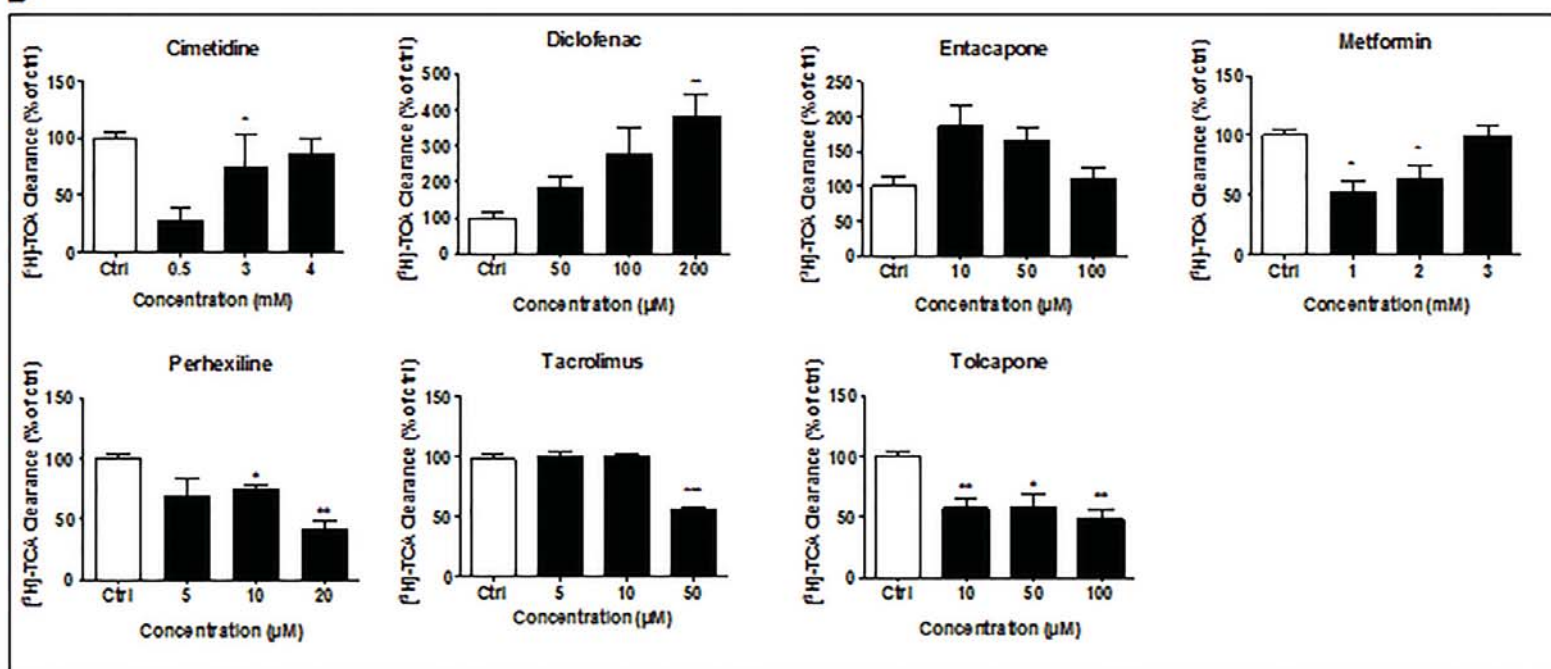
Fig. 3



A



B



C

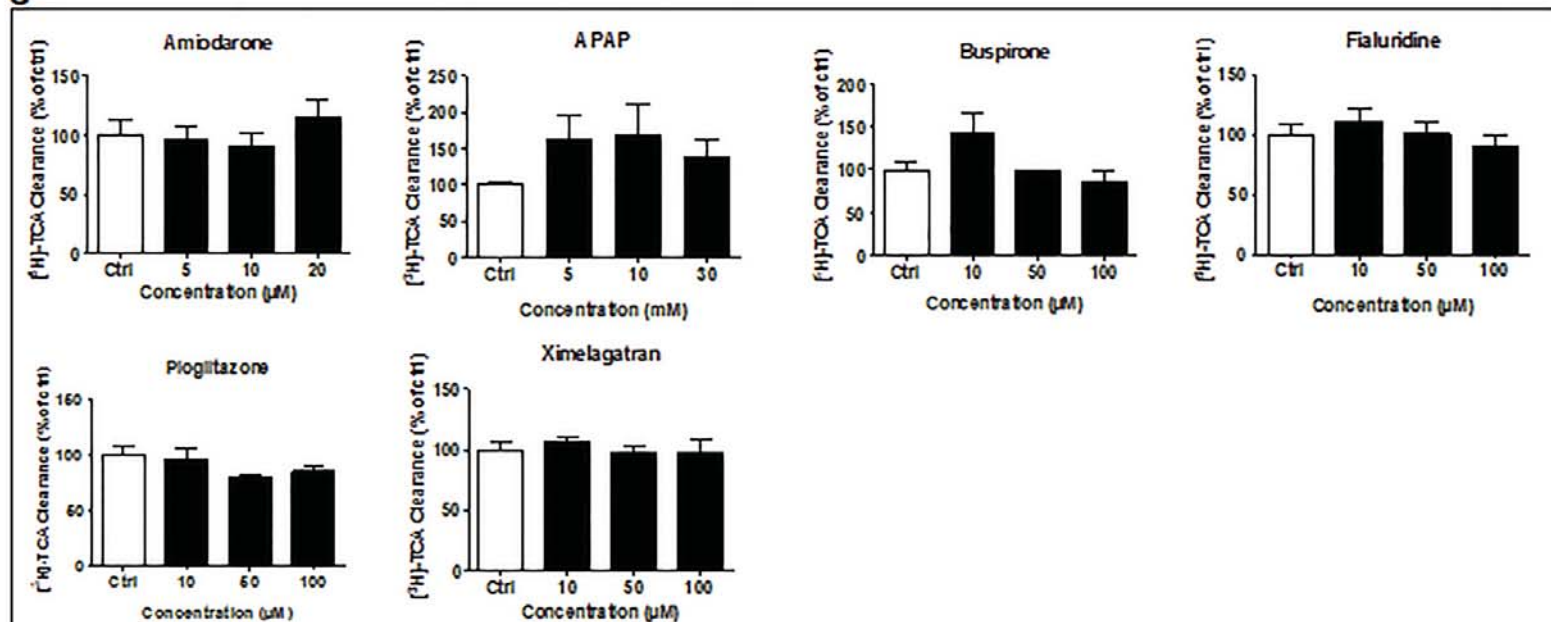
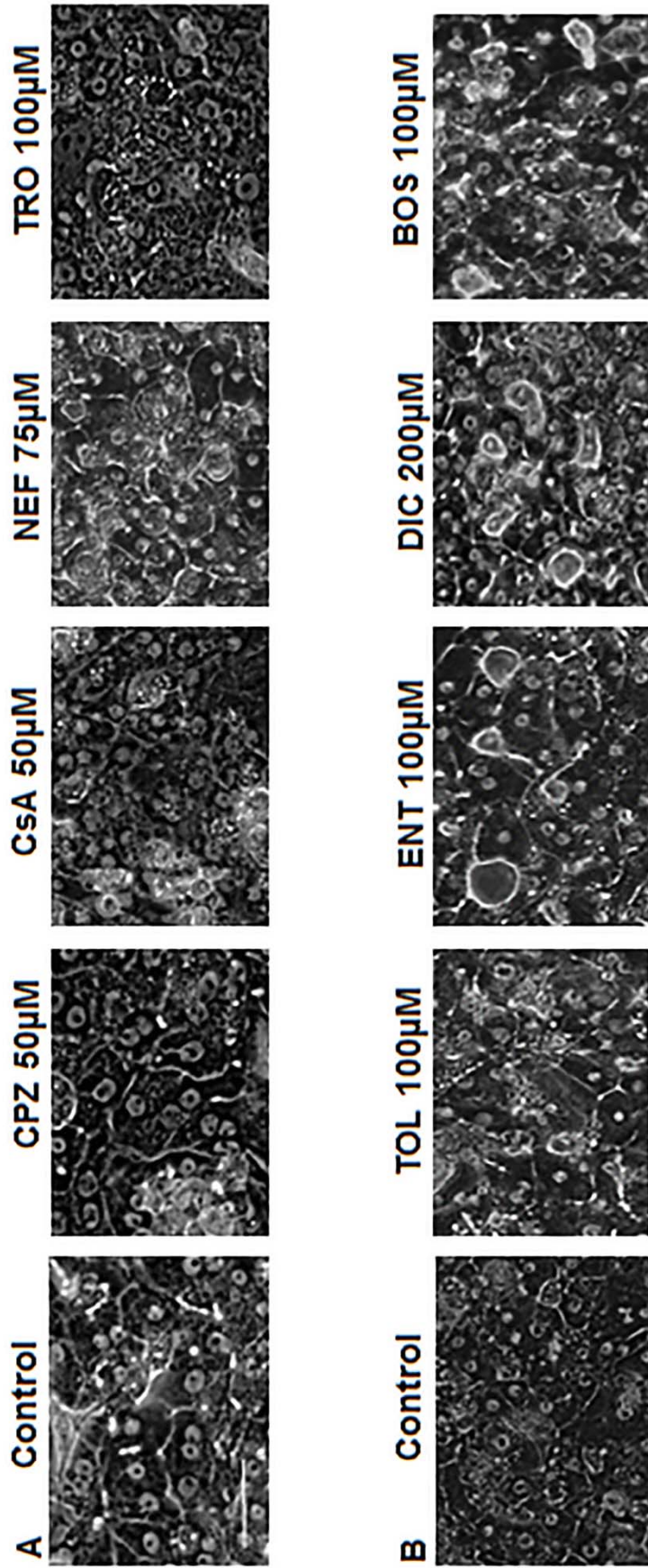


Fig. 5



C

	Donor 1	Donor 2	Donor 3
NEF	constriction	constriction	constriction
DIC	dilatation	dilatation	nc
PER	nc	nc	nc
TRO	constriction	constriction	constriction
ENT	dilatation	nc	dilatation
TOL	dilatation- constriction	dilatation- constriction	dilatation- constriction
FIA	nc	nc	nc

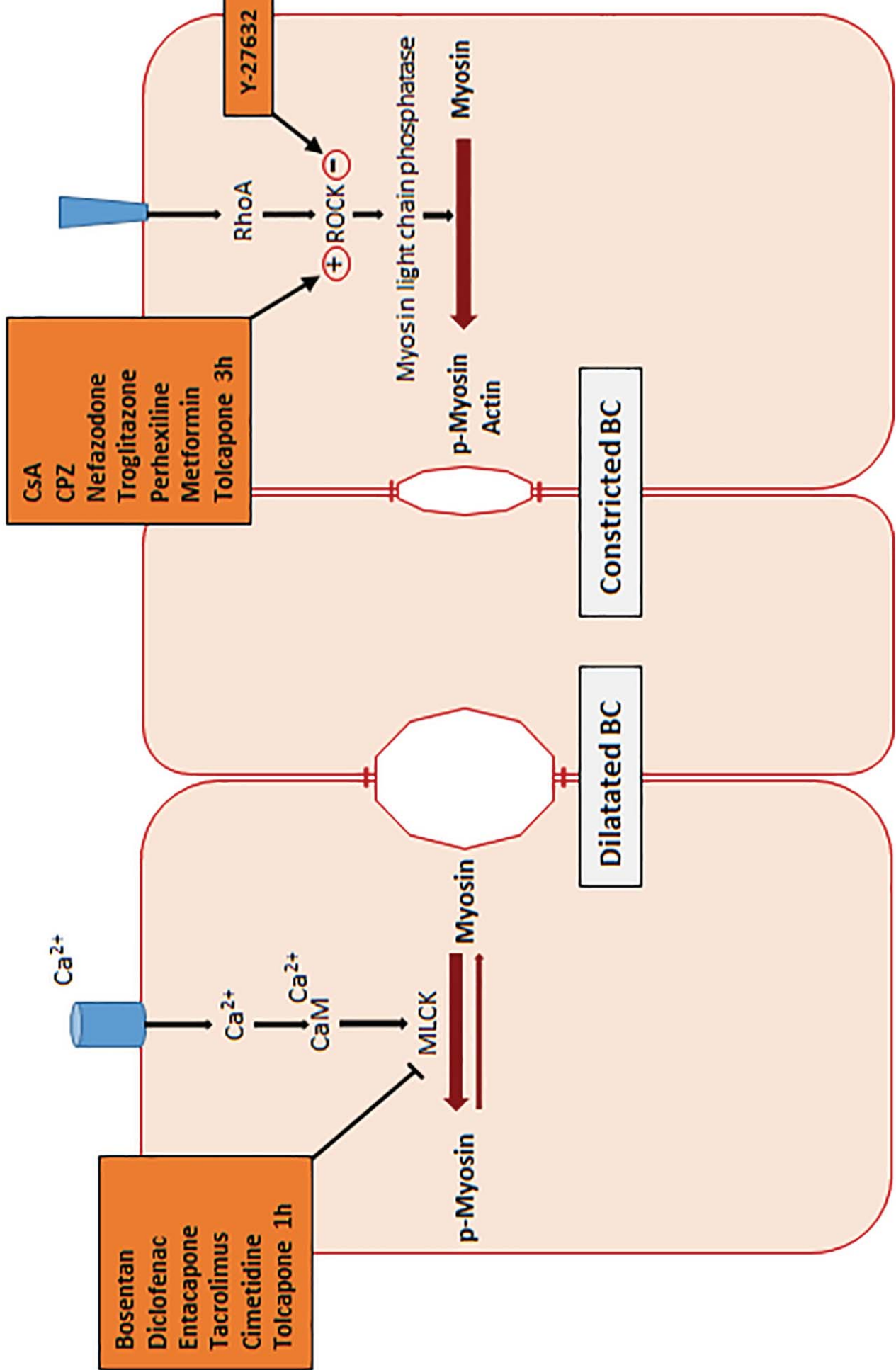


Fig. 6

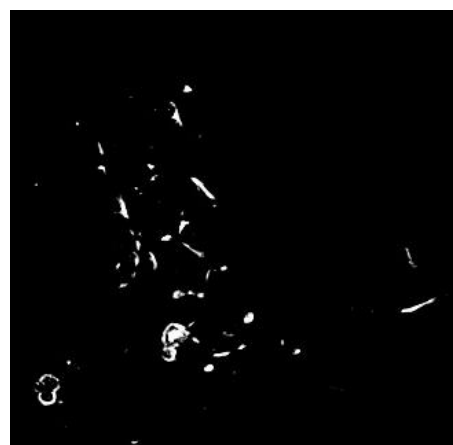
Drug Metabolism and Disposition

Early alterations of bile canaliculi dynamics and the ROCK/MLCK pathway are characteristics of drug-induced intrahepatic cholestasis

Matthew G. Burbank, Audrey Burban, Ahmad Sharaneq, Richard J. Weaver, Christiane Guguen-Guillouzo, André Guillouzo

Supplemental Figure. 1.

A

CsA 50 μ M (CONSTRICTION)

Integrated density

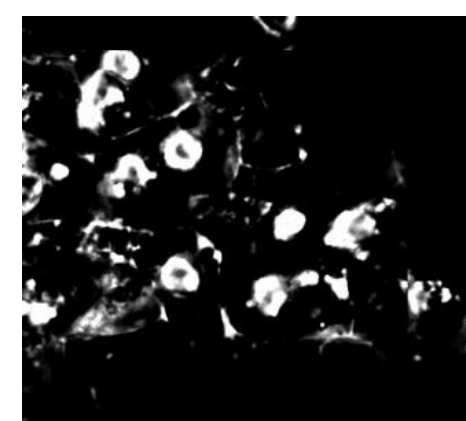
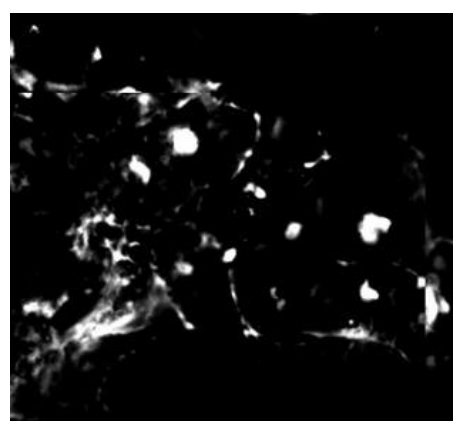
8629394

6856399

% white surface

100%

79.4%

ENT 100 μ M (DILATATION)

Integrated density

29518021

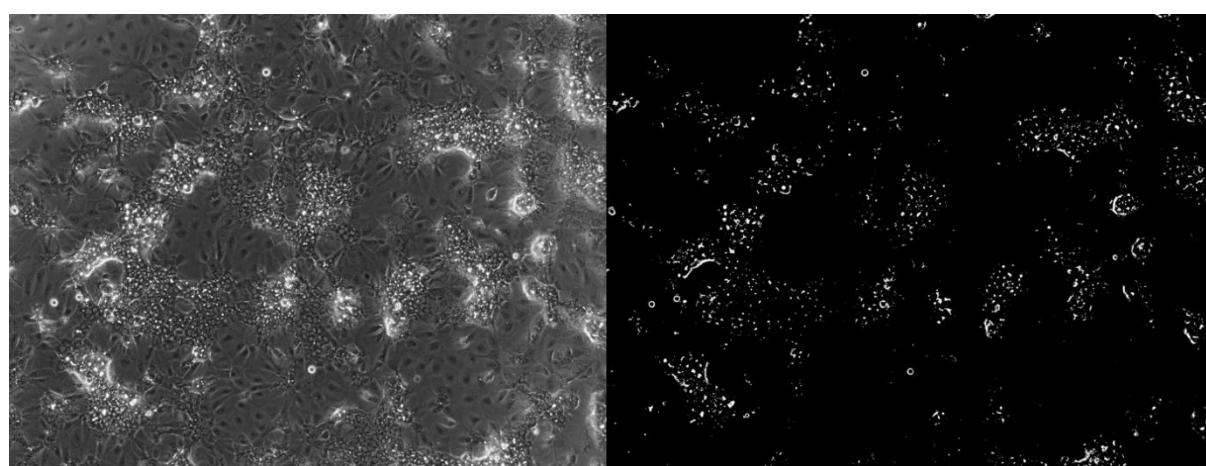
41731151

% white surface

100%

141.3%

B



Phase-contrast photograph

Density adjustment

Supplemental Figure. 1. Method for BC constriction/dilatation quantification

(A), Cells were treated with 50 μ M CsA (constriction) or 100 μ M ENT (dilatation) for 2h. Canalicular lumen surfaces appeared bright (white) and hepatocytes/biliary cells denser (black) using a phase-contrast microscope Zeiss Axiovert 200M. Brightness parameters were adjusted to eliminate non corresponding objects and analysis was performed on at least 4 images per each condition (well). White canalicular lumen was then quantified using the image J software every 10min for 24h. The integrated density was determined and then expressed as percent of the control (T0). (B), Differences between a phase-contrast photograph and the same photograph after density adjustment.

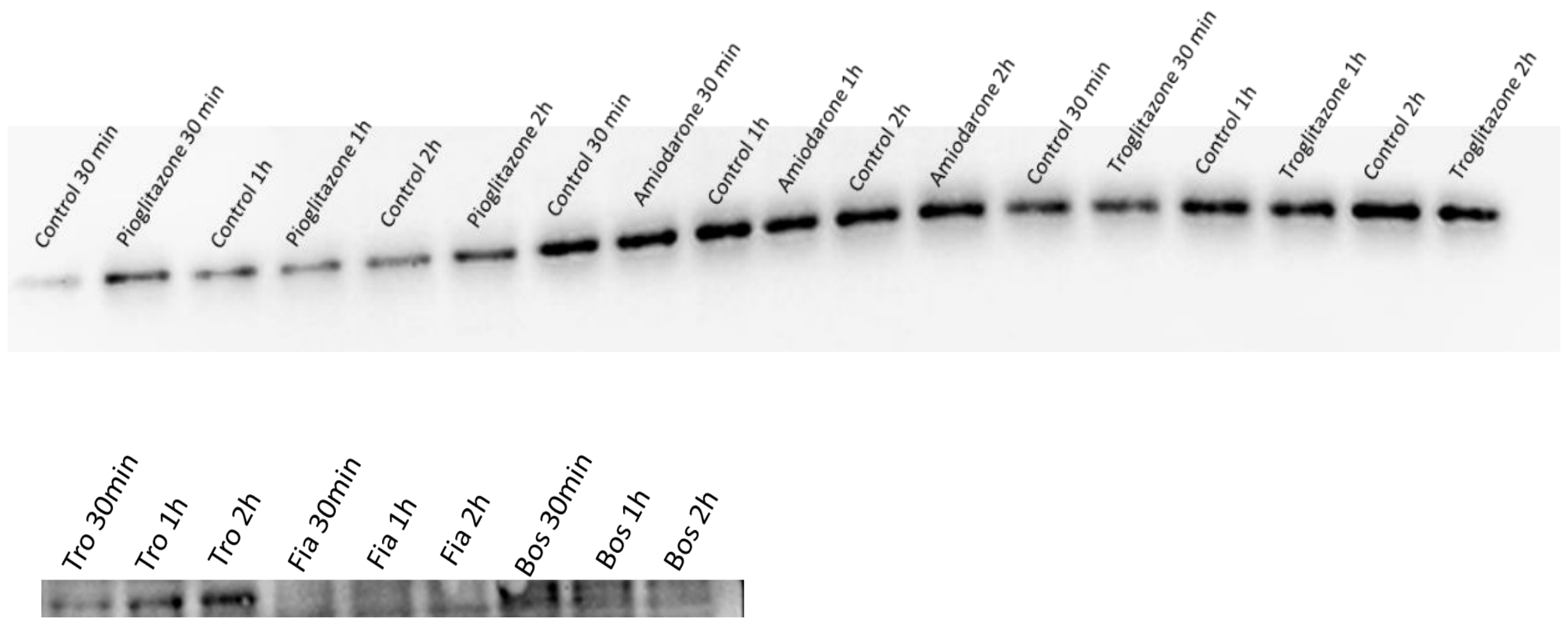
Supplemental Table 1.

	Drugs
BC dilatation	BOS, DIC, ENT, TAC, CIM
BC constriction	CPZ, CsA, NEF, TRO, PER, MET
BC dilatation then constriction	TOL
No effect on BC	AMI, APAP, BUS, FIA, PIO, XIM

Supplemental Table 1. Drug-induced BC modulations

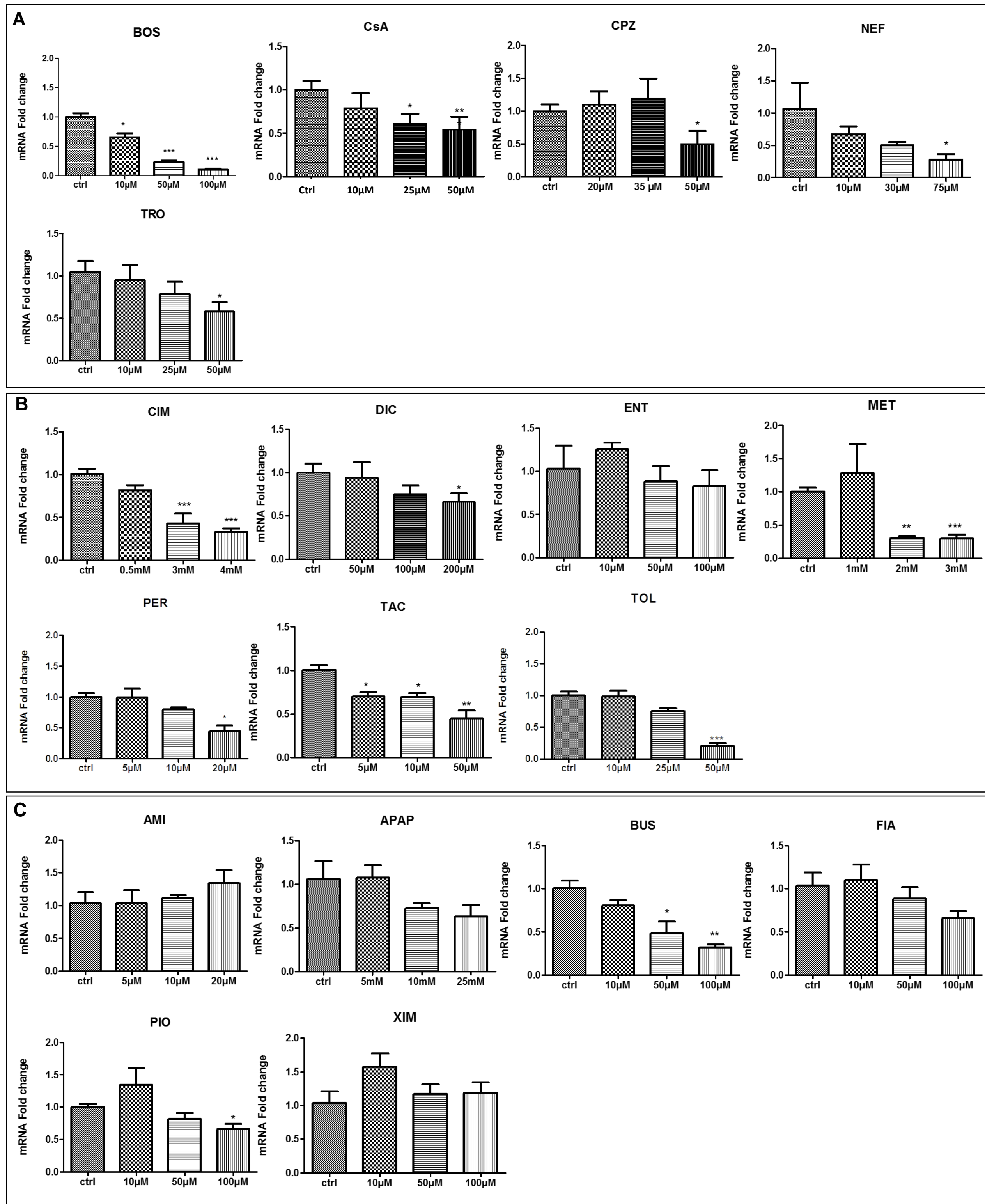
AMI, amiodarone; APAP, acetaminophen; BOS, bosentan; BUS, buspirone; CIM, cimetidine; CPZ, chlorpromazine; CsA, cyclosporine A; DIC, diclofenac; ENT, entacapone; FIA, fialuridine; MET, metformin; NEF, nefazodone; PER, perhexiline; PIO, pioglitazone; TAC, tacrolimus; TOL, tolcapone; TRO troglitazone; XIM, ximelagatran.

Supplemental Figure. 2.



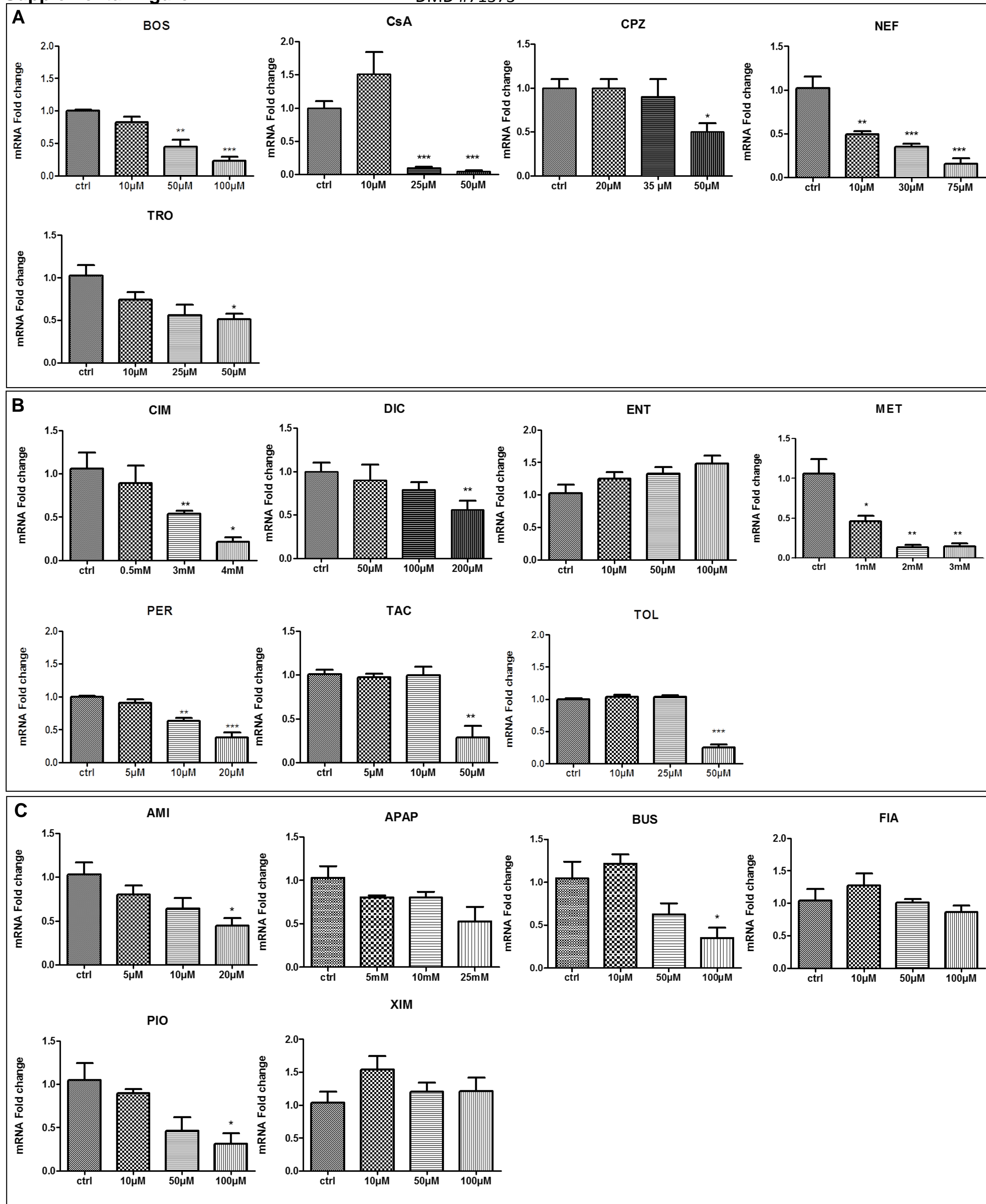
Supplemental Figure. 2. Comparative effects of a 30min versus longer times treatment with various tested drugs on MLC2 phosphorylation/dephosphorylation activity in HepaRG cells.

Representative western blots of p-MLC2 using anti-S19 phospho MLC2 antibody, at various time points (30min, 1h and 2h) in cells treated with 6 cholestatic and non cholestatic drugs, i.e. 100 μ M PIO (non cholestatic), 20 μ M AMI (non cholestatic), 50 μ M TRO (cholestatic, bile canaliculi constrictor), 100 μ M FIA (non cholestatic) and 100 μ M BOS (cholestatic, bile canaliculi dilatator). Alterations of MLC2 phosphorylation are similar after 30min whatever the compound.



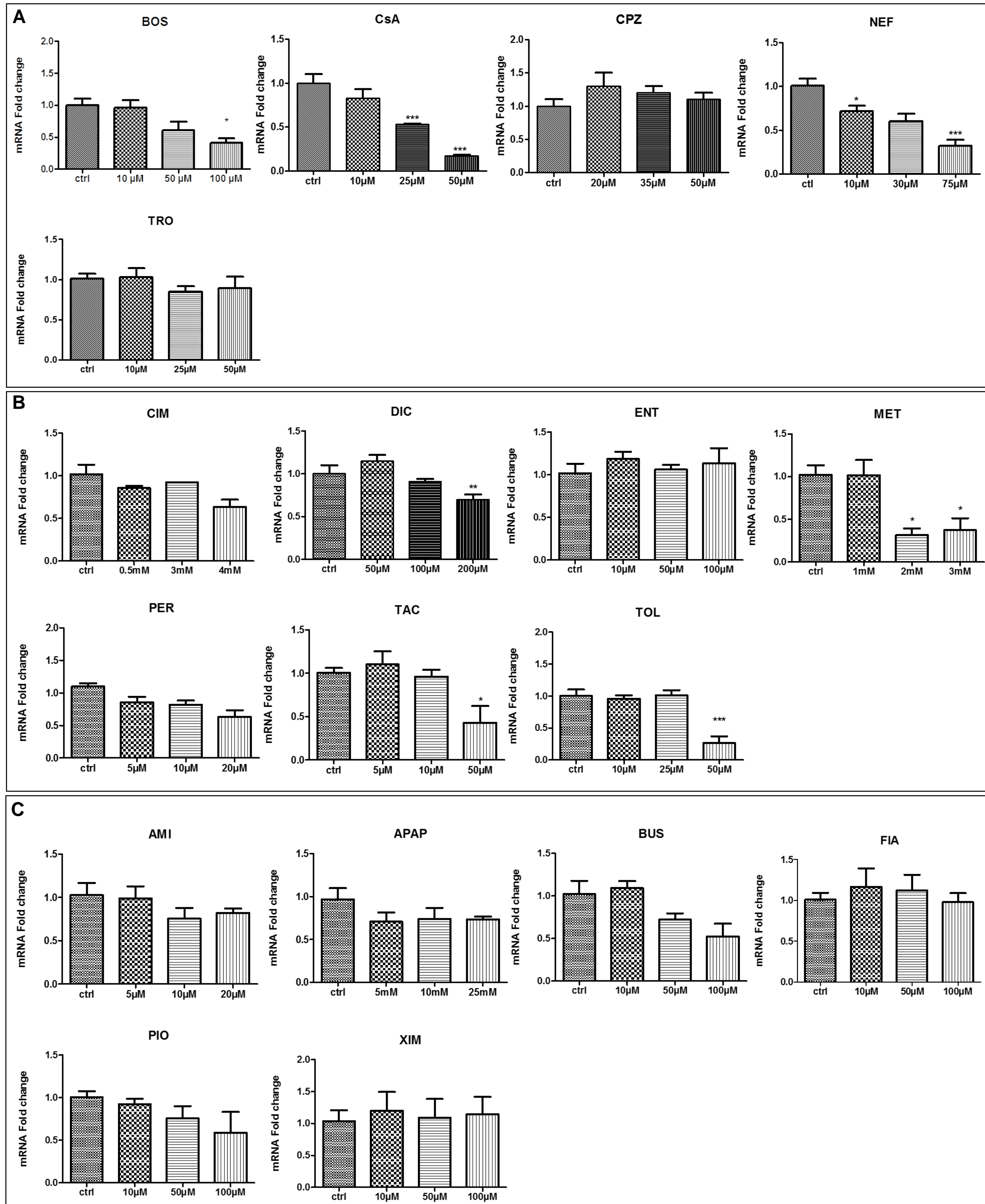
Supplemental Figure. 3. Effects of the tested drugs on BSEP transcript levels

HepaRG cells were exposed to the 3 groups of compounds at 3 different concentrations for 24h : group 1 (A), group 2 (B) and group 3 (C). mRNA levels of BSEP were measured by RT-PCR analysis. All results are expressed relative to the levels found in control cells (ctrl), arbitrarily set at a value of 1. * $P < 0.05$, ** $P < 0.01$ and *** $P < 0.001$ compared with untreated cells.



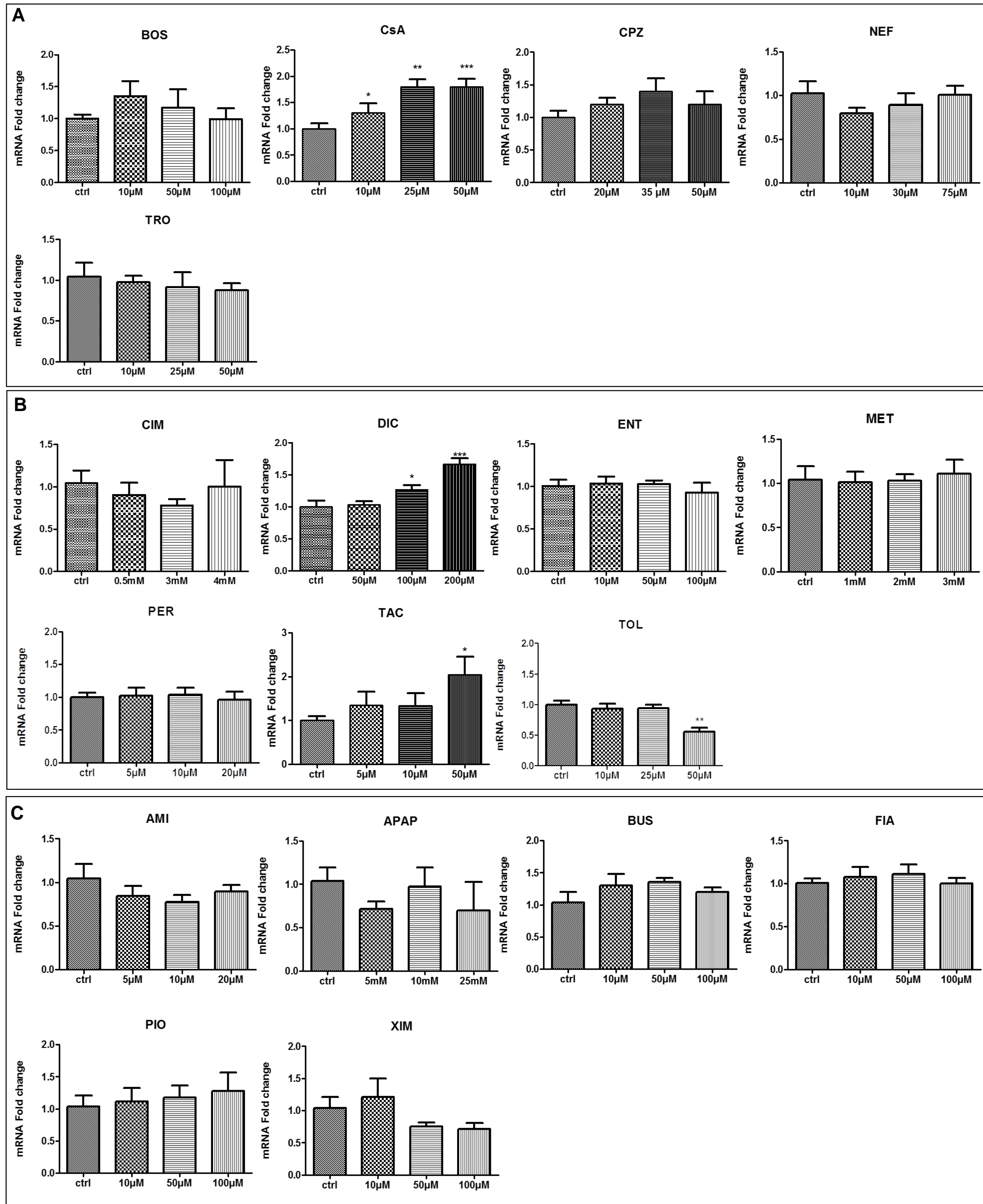
Supplemental Figure. 4. Effects of the tested drugs on NTCP transcript levels

HepaRG cells were exposed to the 3 groups of compounds at 3 different concentrations for 24h : group 1 (**A**), group 2 (**B**) and group 3 (**C**). mRNA levels of NTCP were measured by RT-PCR analysis. All results are expressed relative to the levels found in control cells (ctrl), arbitrarily set at a value of 1. * $P < 0.05$, ** $P < 0.01$ and *** $P < 0.001$ compared with untreated cells.



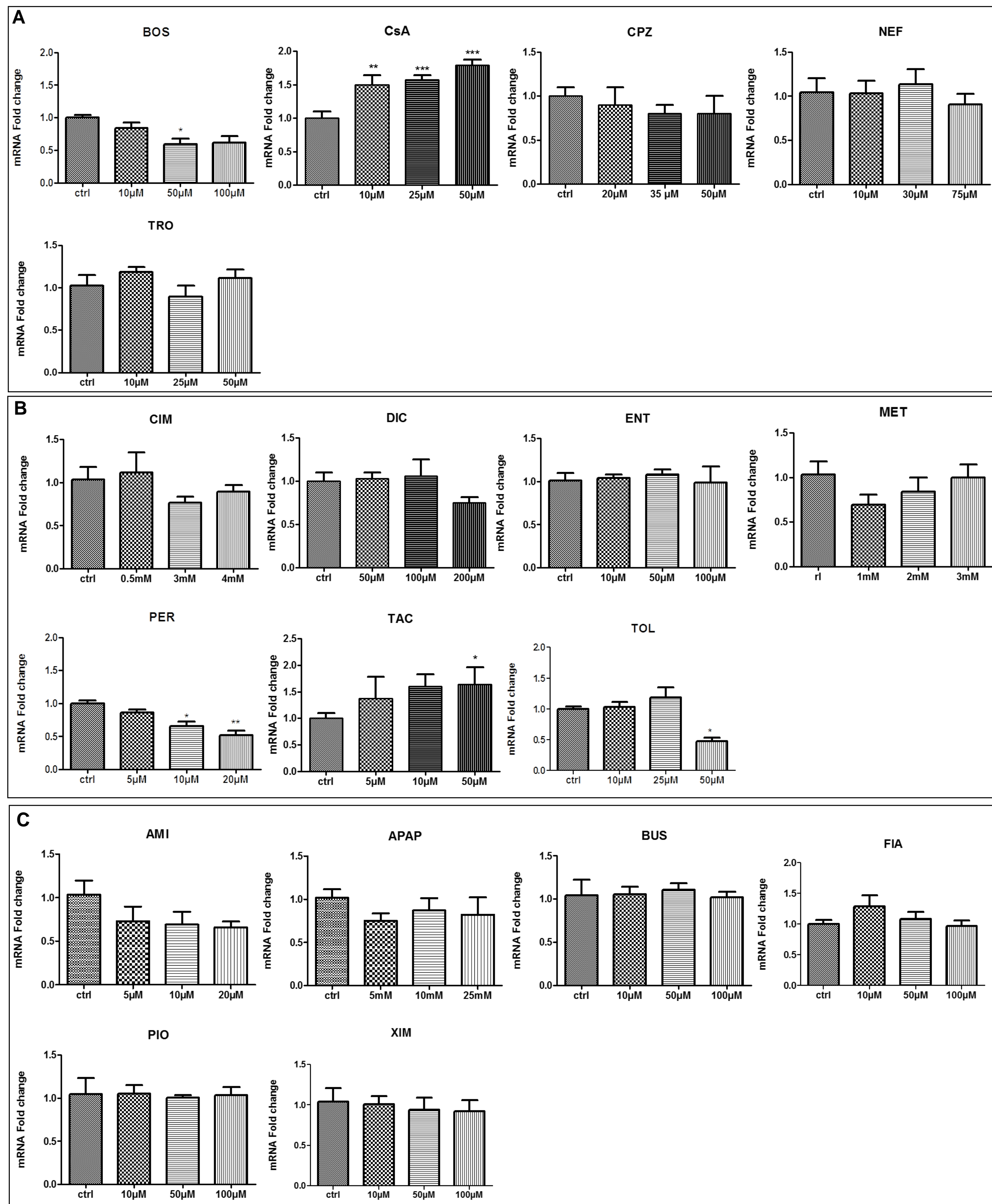
Supplemental Figure. 5. Effects of the tested drugs on OATP-B transcript levels

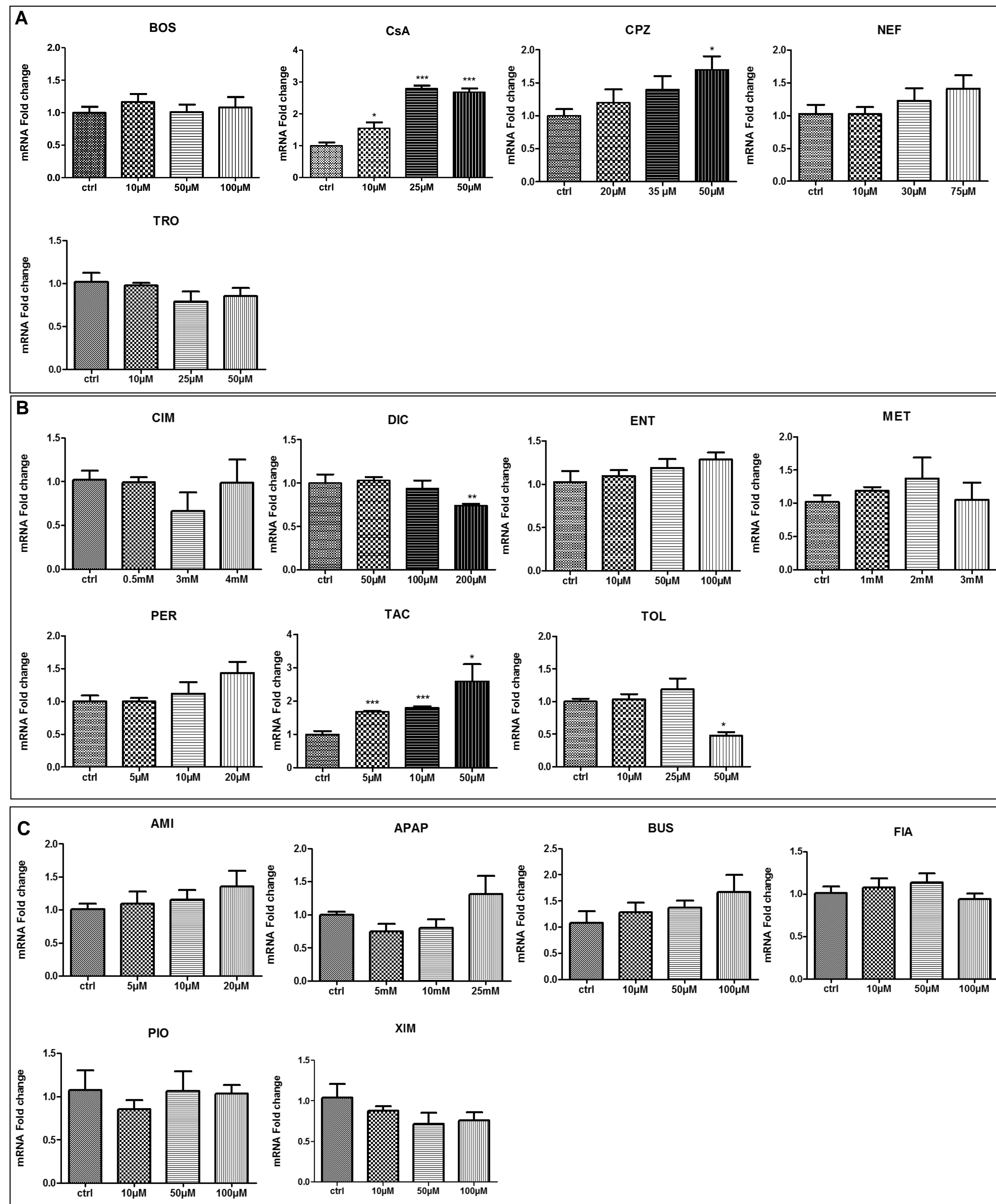
HepaRG cells were exposed to the 3 groups of compounds at 3 different concentrations for 24h : group 1 (A), group 2 (B) and group 3 (C). mRNA levels of OATP-B were measured by RT-PCR analysis. All results are expressed relative to the levels found in control cells (ctrl), arbitrarily set at a value of 1. * $P < 0.05$, ** $P < 0.01$ and *** $P < 0.001$ compared with untreated



Supplemental Figure 6. Effects of the tested drugs on MRP2 transcript levels

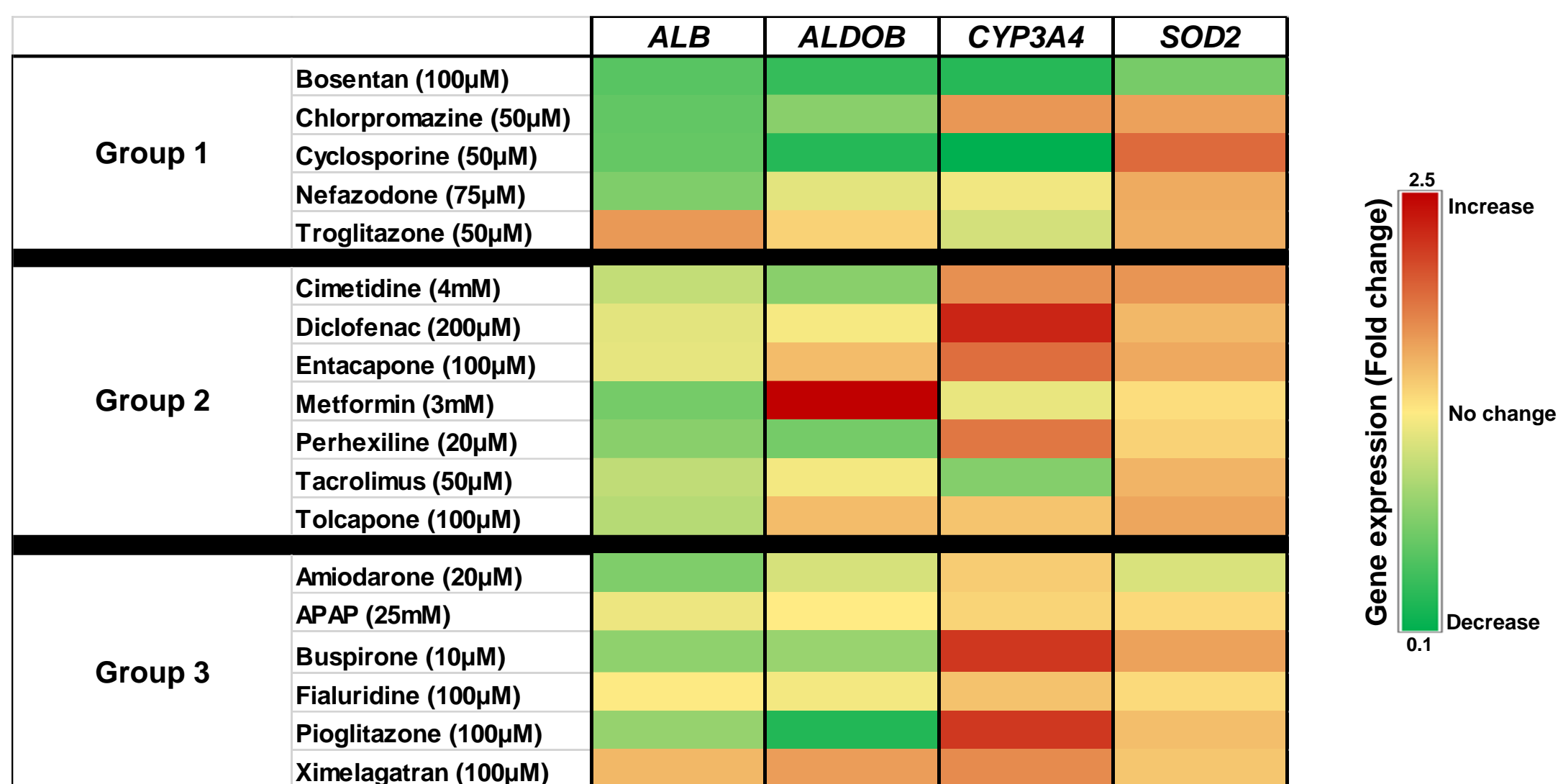
HepaRG cells were exposed to the 3 groups of compounds at 3 different concentrations for 24h : group 1 (A), group 2 (B) and group 3 (C). mRNA levels of MRP2 were measured by RT-PCR analysis. All results are expressed relative to the levels found in control cells (ctrl), arbitrarily set at a value of 1. * $P < 0.05$, ** $P < 0.01$ and *** $P < 0.001$ compared with untreated cells.





Supplemental Figure. 8. Effects of the tested drugs on MRP4 transcript levels

HepaRG cells were exposed to the 3 groups of compounds at 3 different concentrations for 24h : group 1 (A), group 2 (B) and group 3 (C). mRNA levels of MRP4 were measured by RT-PCR analysis. All results are expressed relative to the levels found in control cells (ctrl), arbitrarily set at a value of 1. * $P < 0.05$, ** $P < 0.01$ and *** $P < 0.001$ compared with untreated cells.



Supplemental Table. 2. Heat map showing the effects of the tested drugs on transcript levels of non transporters genes

HepaRG cells were exposed to the 3 groups of compounds at 3 different concentrations for 24h : group 1, group 2 and group 3. mRNA levels of *ALB*, *ALDOB*, *CYP3A4*, *SOD2* were measured by RT-PCR analysis. All results are expressed relative to the levels found in control cells, arbitrarily set at a value of 1. two colors are used : Red when there is an increase in the fold change of gene expression and green when there is a decrease in the fold change of gene expression

Supplemental Video 1. Constriction of BC in troglitazone-treated HepaRG cells

Constriction of BC and loss of their rhythmic dynamics in TRO-treated HepaRG cells. Images of 50 μ M TRO-treated cells were captured each 10 minutes during 24h under time-lapse phase-contrast videomicroscopy equipped with a thermostatic chamber (37°C and CO₂).

Supplemental Video 2. Dilatation of BC in entacapone-treated HepaRG cells

Dilatation of BC and loss of their rhythmic dynamics in ENT-treated HepaRG cells. Images of 100 μ M ENT-treated cells were captured each 10 min during 24h under time-lapse phase-contrast videomicroscopy equipped with a thermostatic chamber (37°C and CO₂).

Supplemental Video 3. BC rhythmic dynamics movements in acetaminophen-treated HepaRG cells

Rhythmic dynamics movements in APAP-treated HepaRG cells. Images of 25mM APAP-treated cells were captured each 10 min during 24h under time-lapse phase-contrast videomicroscopy equipped with a thermostatic chamber (37°C and CO₂).